Altered rock spectra in the visible and near infrared

by

Graham R. Hunt[1] and Roger P. Ashley[2]

[1]U.S. Geological Survey, Denver, Colorado 80225

[2]U.S. Geological Survey, Menlo Park, California 94025

ABSTRACT

Visible and near-infrared (0.35 to 2.5 μm) bidirectional reflection spectra were recorded for a suite of well-characterized hydrothermally altered rock samples. The spectra typically display well-defined bands caused by both electronic and vibrational processes in the individual mineral constituents.

Electronic transitions in the iron-bearing constituent minerals produce diagnostic minima near 0.43, 0.65, 0.85, and 0.93 μm. Vibrational transitions in clay and water-bearing mineral constituents typically produce characteristic single or multiple features over limited spectral ranges near 1.4, 1.75, 1.9, 2.2, and 2.35 μm. The most abundant feature-producing minerals present in these rocks are hematite, goethite, and alunite, while others frequently present are jarosite, kaolinite, potassium micas, pyrophyllite, montmorillonite, diaspore, and gypsum.

This study shows that visible-near infrared spectrometry is a reliable and rapid technique for detecting and identifying clay minerals and alunite in rocks. Because these minerals are important constituents of altered rocks, the feasibility of using the visible and near infrared for detecting altered rocks by remote-sensing techniques is indicated. The spectral region near 2.2 μm is particularly important for this purpose.

INTRODUCTION

The visible and near-infrared bidirectional reflection spectra (0.35 to 2.5 μm) of a suite of hydrothermally altered rocks were recorded using a Cary Model 14* spectrophotometer and a prototype attachment designed to accomodate particulate and solid samples in a horizontal plane so that their upper surfaces could be inspected (Hunt and Ross, 1967).

The samples were collected by one of us (R.P.A.), who performed mineralogical analyses of each using optical and X-ray petrographic techniques to identify all the constituent minerals. The samples were then classified according to the type of alteration that had occurred, namely: silicified, advanced argillic, montmorillonitic argillic, phyllic, or advanced phyllic; plus some samples that displayed opaline or other types of alteration (Meyer and Hemley, 1967).

The purposes of this study are to show that several common alteration minerals have abundant spectral features in the 0.4-2.5 μm** region, making laboratory reflectance infrared techniques useful for the study of altered rocks, and to show that most of these spectral features are available with natural illumination, indicating that remote-sensing methods for mapping variations in hydrothermally altered rocks are feasible in this spectral region.

---

* Any use of trade names or trademarks in this publication is for descriptive purposes only and does not constitute endorsement by the U.S. Geological Survey.

** μm = micrometers

In the figures presented here, the rock spectra are assembled into separate diagrams for each of the major alteration types listed above, together with a group labeled "miscellaneous". Within each of these figures the spectra of the samples have been arranged initially according to spectral similarity in the near-infrared range (from 1.2 to 2.5 μm). It is apparent that the features in each spectrum can be explained in terms of those of the constituent minerals of the rock sample.

In each group of spectra, it is also fairly obvious that typically the features of one constituent mineral (usually a clay mineral) dominate the spectrum from 1.2 to 2.5 μm. A similar situation pertains to the wavelength range short of 1.2 μm, where the spectrum is dominated by the features of a few iron-bearing minerals.

Of the constituent minerals listed, some (such as quartz and the feldspars, for example) do not produce any features over the range investigated, so they do not contribute any features to the total rock spectrum.

Some of the most characteristic features of alteration minerals occur near 1.4 and 1.9 μm, two regions that are obscured by atmospheric absorption, so they are of no use for conventional terrestrial remote-sensing techniques that use solar energy as the radiation source. However, these regions could prove extremely useful for active remote-sensing and analytical techniques, so the features that occur are discussed in some detail.

Spectral features that occur in altered rocks derive from both electronic and vibrational processes, principally involving iron or the

hydroxyl group, and these processes will be discussed initially in reference to the spectra of the constituent minerals.

FIELD SAMPLING AND LABORATORY PROCEDURES

Western Nevada was chosen for a series of Landsat studies of hydrothermally altered rocks because altered areas are numerous and easily accessible, and vegetation is sparse except at higher elevations (Rowan and others, 1974; Rowan and others, 1977; Abrams and others, 1977). In the course of these studies, field spectral reflectance measurements were made in several hydrothermally altered areas (see fig. 1 and table 1), and samples collected for the mineralogical information necessary to interpret the field spectra. This suite of samples provides the geological materials for this study, which in turn confirms spectral results obtained in the field. Prior studies have included spectral reflectance measurements of various alteration minerals (Hunt and Salisbury, 1970, 1971; Hunt and others, 1971a, b, 1973) and measurements of altered rocks in situ (Rowan and others, 1977), but the mineralogies of the altered rocks studied in the laboratory were not examined in the detail of those in the present study nor with quite such a high spectral resolution instrument. This study represents an attempt to partly fill this gap.

The sites providing samples for this study are all outcrops or monolithologic talus with little or no soil. Laboratory and field spectral reflectance results are best compared at these sites because the chances of obtaining a field sample unrepresentative of the field of view of the

field spectrophotometer are minimized. The hydrothermally altered areas studied, however, are dominated by clay-bearing rocks which are mostly poorly to moderately well exposed, and include few large outcrop areas. The most common surface material consists of rock fragments with various amounts of soil. Thus, our collection is probably somewhat biased toward more clay-poor altered rocks than are typical of these areas.

Chips totaling 1-3 cm^3 in volume were ground to pass a Tyler 200-mesh screen (opening 74 μm). This material was placed in an aluminum cell pack for X-ray diffraction analysis. To improve clay-mineral identification for many samples, a small amount of sample was removed and dispersed in water with an ultrasonic probe. Suspension containing particles smaller than about 5 μm was dried on a glass slide to form a clay-rich residue, treated with ethylene glycol, and heated to 400°C and then to 600°C, with X-ray analysis repeated after each step. The material examined with the modified Cary spectrophotometer was largely identical to that used for the X-ray cell pack for each sample. Because the holders for the two instruments are substantially different, however, and because diffractometry and spectrometry were done in different laboratories in Menlo Park, California, and Denver, Colorado, respectively, the X-ray cell packs were destroyed and the disc-shaped packs for the Carey formed subsequently from the same stock sample powder.

Most samples were examined by optical petrographic methods; the chip used for thin section was taken from the same hand specimen as the X-ray chips whenever possible. Correlation between modal mineral percentages and relative X-ray peak heights is usually good but only if no

more than rough semiquantitative mineral percentages are attempted. Reasons for differences between optical and X-ray petrographic estimates include sample inhomogeneities, difficulties in identifying fine-grained material for optical point-counts, and various complexities involved in making quantitative comparisons of X-ray diffraction data (Tatlock, 1966). In general, optical estimates are more precise and accurate than X-ray estimates, but because our spectral reflectance data are for the rock portions examined by X-ray rather than by optical petrography, we present semiquantitative modal data only. In the coded mineral assemblage accompanying spectral data given for each sample, mineral components are listed in order of decreasing abundance, with components present in amounts less than about 10 percent enclosed in parentheses.

CLASSIFICATION OF ALTERED ROCKS

The rocks studied here are mainly quartz with various mixtures of the following minerals: kaolinite, montmorillonite, diaspore, pyrophyllite, opal, potassium mica (K-mica), potassium feldspar (K-feldspar), plagioclase, and alunite. The most common minor constituent is leucoxene (fine-grained rutile or anatase). Before oxidation took place near the weathering surface, most rocks contained pyrite, which is now replaced by various mixtures of jarosite, goethite, and hematite. Table 2 is a complete list of minerals found and the abbreviations assigned to them for use in later figures.

Our usage of names for altered rocks is generally the same as that of Meyer and Hemley (1967). Table 3 summarizes guidelines used here in applying these names. Generally, this classification is appropriate

for grouping rocks with respect to spectral behavior, because many clay minerals, alunite, and pyrophyllite have important and diagnostic spectral features in the visible-near infrared wavelength region. The only addition to established nomenclature that we have made in this study is the term "advanced phyllic", which we apply to rocks with the assemblage quartz-K mica-alunite. With appearance of any kaolinite or pyrophyllite, a rock with these three minerals is termed "advanced argillic", but rather than being a scarce end-member assemblage, substantial volumes of advanced phyllic rocks exist in some of the altered areas we studied.

Dominant iron mineral provides a logical secondary basis for classification, because iron minerals strongly affect the 0.4-1.1 μm portion of the visible-near infrared region in diagnostic ways. Thus, in one set of figures presenting spectral reflectance data, the samples are grouped by major iron mineral and approximate abundance of iron minerals. Again, a mineral is considered abundant, if present in an amount greater than approximately 10 percent.

MINERAL SPECTRA

Electronic Processes

In the altered rock spectra discussed here, all features that appear at wavelengths shorter than about 1.2 μm are due to various electronic transitions involving iron. Figure 2 shows the spectra of typical altered rock constituent minerals in the range 0.35 to 1.5 μm.

Two general types of transition may occur. Those that involve the transfer of an electron between two ions, called intervalence charge

transfer (IVCT) transitions, occur between the ions of two different elements (usually the ferric and oxygen ion) or between different ions of the same elements (as, for instance, between ferric and ferrous ions). The IVCT transitions are characterized by extremely intense absorptions. The second type of transition occurs between the crystal or ligand field perturbed energy levels of an ion. The location and intensity of the spectral features for a particular ion will therefore depend upon the nature and intensity of the perturbing field. For altered rock spectra, features may be caused by crystal field transitions (CFT) in ferric ions.

The exact interpretation of the iron spectra in minerals is still not complete. However, the most intense absorption for ferric oxide materials occurs for the IVCT transition and the band that it produces has its center in the near-ultraviolet range, so that only one side of the feature extends into the visible range. In the iron oxides, it is this mechanism that produces the rapid fall-off in reflected intensity to shorter wavelengths, and this fall-off is apparent in the goethite and hematite spectra. Overlying this intense absorption are features due to the ferric ion crystal field transitions. There are typically three fairly broad features that occur in the oxides due to the CFT's: the $6A_1 \rightarrow {}^4A_{1g}$ that occurs between 0.75 and 0.95 μm; and the $6A_1 \rightarrow {}^4A_{2g}$ that appears between 0.55 and 0.65 μm, usually as a shoulder; and the $6A_1 \rightarrow {}^4A_1$, ${}^4E(G)$ that appears near 0.45 μm. The latter feature, when it is observable (which it rarely is, because it lies beneath the intense IVCT) should shift less than the other two features because it is field independent.

In hematite, the $6A_1 \rightarrow {}^4T_{1g}$ is clearly centered near 0.85 μm, while for the sample of goethite, it is centered at almost 0.1 μm longer wavelength, near 0.94 μm. The shoulder near 0.65 μm, $6A_1 \rightarrow {}^4A_{2g}$ is most apparent in goethite.

As stated above, the $6A_1 \rightarrow {}^4A_1$, $^4E(G)$ feature near 0.45 μm is usually not discernible, but with jarosite this feature is clearly apparent as an unusually sharp band near 0.43 μm. The enhanced intensities of spin-forbidden bands have recently been explained as antiferromagnetic coupling among the Fe^{3+} ions in materials that contain extended two-dimensional hydroxo-bridged Fe^{3+} sheets, such as in jarosite (Rossman, 1976). Manning (1973) had previously suggested from a study of extinction coefficients of Fe^{3+} bands in silicates and oxides that an intensity-stealing mechanism is operating such that the states involving spin-forbidden ligand field transitions mix with nearby states that involve spin-allowed oxygen-metal charge transfer transitions, especially apparent in oxides.

The presence of the ferrous ion as opposed to the ferric ion is most typically evidenced by the prominent appearance of a broad band near 1 to 1.1 μm, due to the spin-allowed transition between the E_g and T_{2g} levels into which the D ground state splits in an octahedral field. Other weak features due to spin-forbidden Fe^{2+} transitions occur near 0.43, 0.45, 0.51, and 0.55 μm, while the 1.0 μm feature is accompanied by broad features to longer wavelengths near 1.8 μm in some silicates.

Vibrational Processes

Figure 3 shows the 0.6 to 2.5 μm spectra of a selection of typical

altered rock constituent minerals. From 1.2 μm to longer wavelengths, all features displayed exclusively involve vibrational transitions of the hydroxyl (OH) groups. In several respects these spectra are quite similar to each other, and where they differ they do so because unique features appear.

All the spectra display single or multiple features at or within 0.1 μm to 1.4 μm. In every case, these features are due to the first overtone of the fundamental OH-stretching vibration, or to a combination of the fundamental stretching modes of two different OH groups, and the features occur near here regardless of whether the OH is attached to H, Si, Al, or Mg. For multiple features to occur, there must be two or more different OH-group types present, different because they exist in somewhat different environments.

Even though the 1.4 μm feature is common to all OH-bearing minerals, its exact appearance and location varies sufficiently from mineral to mineral to allow some discriminations to be made. For example, in phlogopite the single feature lies to shorter wavelengths than in lepidolite, muscovite, montmorillonite, and pyrophyllite, all of which also display a well-defined single minimum. In pyrophyllite, the feature is most sharply defined. If more than one feature occurs near 1.4 μm in these materials, the additional band is usually due to the presence of a small amount of another mineral of this group as an impurity.

Materials that display single features near 1.4 μm can be readily distinguished from those that show two or more well-resolved features, such as occur in kaolinite and alunite, and these latter can be dis-

criminated from each other because the kaolinite bands both occur at shorter wavelengths than those in alunite. Additional weaker features that occur in this region are due to more complicated combination overtones of other vibrations.

Most of the spectra shown in figure 3 display a feature or bands near 2.2 μm, and this is due to combinations of the OH-bond fundamental stretch with the Al-O-H fundamental bending mode. Again, these features appear slightly different in different materials, being either sharp (as in pyrophyllite), broad (as in muscovite, montmorillonite), or multiple (as in kaolinite, alunite) with their minima shifting over a range from about 2.16 to 2.23 μm. It is common for this particular feature to appear in phyllosilicates that possess a dioctahedral structure that allows the Al-O-H bend-OH-stretch combination to occur. The feature at 2.2 μm is usually associated with a second prominent, but weaker feature removed about 0.1 μm to longer wavelengths, near 2.3 μm, that is also associated with the presence of aluminum (see alunite).

However, when a feature appears near 2.3 μm in the absence of one at 2.2 μm, it is typically due to a combination of the OH-stretching mode with the bending fundamental of Mg-O-H, and this is illustrated by phlogopite. Again, this feature is usually accompanied by a prominent but less intense feature removed 0.1 μm to longer wavelengths. These features occur in phyllosilicates that possess the trioctahedral structure, but they are also displayed intensely in the spectra of magnesium-bearing amphiboles.

Features at wavelengths longer than 2.4 μm can be assigned to

vibrations involving the OH-stretching modes with the low-lying lattice modes or to fundamental vibrations.

Two further features in these spectra require mention. Hydroxyl groups present in the form of molecular water, no matter how they are attached or included, always produce a feature near 1.9 μm due to the combination of OH with the H-O-H bending fundamental, and this is well illustrated by the montmorillonite spectrum. Montmorillonite is the only mineral of this group that readily absorbs water from the air.

One of the most interesting and commonly occurring features in the rock spectra is well illustrated in the alunite spectrum which displays a very intense band near 1.77 μm. This can be assigned as a combination of the fundamental stretch with the first overtone of the Al-O-H band. This band occurs in a range that is typically devoid of absorption in almost all rock materials (exceptions are gypsum and jarosite) so that it provides an excellent diagnostic tool. Of the other materials that display the 2.2 μm feature, only diaspore gives any indication of displaying strong absorption in the 1.75 μm region, but in diaspore the feature is barely resolved even though it shows generalized intense absorption over the entire 1.65 to 2.5 μm range. This occurs largely because there is extensive hydrogen bonding occurring in this material which causes extensive broadening of the features shown here.

ROCK SPECTRA

Partial spectra (0.35 to 1.4 μm) of the particulate rock samples are shown in figures 5 through 9, and the complete spectra (from 0.35 to 2.5 μm) are shown in figures 10 through 15, where they are grouped

according to hydrothermal alteration type. As with the mineral spectra, features caused by different processes will be discussed separately.

Electronic Processes

The spectra shown in figures 5 thorugh 9 were grouped to emphasize similar features that occur as a consequence of the presence of iron in some form or other. The minerals that are responsible for producing such features in the rock spectra are hematite, goethite, jarosite, and montmorillonite.

Of the 94 rock samples investigated, petrographic analyses indicate that only 5 do not contain either hematite or goethite. Of those that do, 27 contain both hematite and goethite, 27 hematite, and 25 goethite. Twenty-two samples contain jarosite, of which seven also contain both hematite and goethite, five hematite, and nine goethite.

More than one feature-producing mineral in a rock produces a spectrum that contains a composite of the features of the individual minerals. However, because the intrinsic intensity of spectral features varies from mineral to mineral, it does not necessarily follow that the features of the most concentrated component mineral will dominate the rock spectrum, although this is very often what happens. In some spectra the features of a less concentrated mineral will dominate those of a more concentrated one and in others a broad feature of one will mask a sharp feature of another. Examples of these effects will become obvious as the spectra are discussed in detail. Individual spectral features are discussed below.

The 0.43 μm(Jarosite) Band

The spectra shown in figure 5 all exhibit a sharp well-defined, but shallow feature, located near 0.43 μm that occurs on the side of a very broad absorption whose minimum is located at wavelengths shorter than 0.43 μm. The 0.43 μm feature is due to the $6A_1 \rightarrow {}^4A_1$, 4E(G) transition in ferric iron in jarosite, and it is enhanced by an intensity-stealing mechanism.

The petrographic and X-ray analyses indicate that 24 of the 94 rock samples studied here contain detectable amounts of jarosite. Of these, only six (T4-11; 109-2-7; 81-8-4; 100-4-1; 23-1-14; and 24-4-10) do not display the 0.43 μm feature in their spectra (shown in figs. 6-9). All except 24-4-10 contain only minor amounts of jarosite (less than 10 percent) and 24-4-10 contains about 10 percent. In all six, goethite and hematite total between about 5 percent and 30 percent. Five of the six samples with advanced argillic alteration contain only minor amounts of jarosite (less than 10 percent) and yet they do display the spectral feature, but in these five samples, goethite and (or) hematite are only present in minor quantities (less than about 5 percent total). Consequently, we believe that the jarosite feature is being masked by the iron oxide absorption in the case of the six samples listed above.

These observations indicate that the presence of a sharp band near 0.43 μm is diagnostic of the presence of jarosite. This band appears to be an extremely sensitive indicator of the presence of jarosite in the absence of iron oxides, but the presence of large quantities of oxides precludes its appearance when only small amounts of jarosite are

present. The change in absolute reflectivity relative to MgO appears to be sensitive to the amount of jarosite present, suggesting further study to determine the feasibility of using the 0.43 μm feature as a quantitative analytical indicator.

The 0.85 μm (Hematite) Band

Figure 6 shows the spectra from 0.35 to 1.4 μm of 20 samples that contain hematite as an important constituent. In 14 of them, hematite is one of the major components, while in the other 6 it ranges from 1 to 9 percent. In addition, goethite is present in nine of these samples, as a major component in three and a minor component in six. Jarosite is present in small amounts in one of the samples, but because of the masking effect of the large quantities of iron oxides, it is one of the six samples discussed above containing jarosite in which the 0.43 μm feature is not observable.

The spectra shown in figure 6 are all quite similar, being characterized by a rise in reflectivity from short wavelengths to a well-defined maximum near 0.75 μm, followed by a broad minimum which is always short of 0.9 μm, but typically it occurs close to 0.85 μm.

Figure 7 includes the spectra of 34 rock samples, all of which contain hematite as a minor component with the exception of two (whose spectra are shown at the bottom, CP-1-12 and CP-1-13) which contain hematite as a major constituent. Twenty-one of the samples contain goethite; in three it occurs as a major component and in the other seventeen as a minor constituent. Five samples also contain jarosite (three as a major, two as a minor component) whose spectra are obvious

because of the appearance of the 0.43 μm feature. Two other samples contain minor amounts of jarosite but do not show the 0.43 μm feature.

The upper 14 spectra display a minimum at wavelengths shorter than 0.9 μm and near 0.85 μm which is characteristic of the presence of hematite. The amount of hematite is less than 10 percent in all these samples. The highest concentrations of hematite (5 to 10 percent) occur in samples L-11, 109-6-3, and CS-1-15 and the lowest (trace to 1 percent) occur in CS-2-3, 45-11-11, 45-11-15, and 45-11-12. Minor amounts of goethite occur in eight of these samples, but goethite exceeds hematite in only 3 samples.

The twelve spectra immediately below the upper 14 display the feature at 0.9 μm or at slightly longer wavelengths. In 7 of these samples there is more goethite than hematite and in 2 samples more hematite than goethite. In three samples (4-29-5F, 45-11-20, and 24-5-9) amounts of hematite and goethite are subequal. Five of these samples contain jarosite. In these 12 spectra, the feature at 0.85 μm typical of pure hematite is apparently beginning to be dominated by those due to other iron-bearing minerals and the minimum is being shifted to longer wavelengths.

Very fine-grained hematite and goethite are often difficult to distinguish optically and impossible to distinguish by whole-rock X-ray diffraction. The anomalous abundance relationships shown by hematite and goethite in a minority of the first 24 samples on figure 7 are probably the result of misidentification of some fine-grained material.

The bottommost eight spectra show barely detectable broad features near 0.9 μm or no absorption features (minima) at all in this range even

though iron-bearing minerals are scarce (only a trace) in only one sample (5-2-I). In fact, the bottom two spectra show a maximum near 0.9 μm which is most unusual. Their mineral content gives no clue as to why their spectra should appear this way, and we have no explanation for it at this time.

The 0.9+ μm (Geothite, Jarosite) Band

In figure 8 is shown the spectra of 19 samples, 17 of which contain goethite. In ten of these it is one of the major components, while in the other seven it is a minor constituent. In nine of these samples hematite is also present but only as a minor component. Hematite is listed as being more abundant than goethite in only one sample (81-4-7), but this particular sample was fragmental and notably heterogeneous, so goethite may be a major component in the portion examined with the Cary.

The other two spectra, shown at the bottom (24-4-3 and 24-4-8), are of samples that do not contain goethite, but both contain jarosite as a major component. Jarosite is also present in seven of the other samples (major component in four samples, minor component in 3 samples).

Figure 9 displays the spectra of 13 samples, all of which contain goethite as a minor component, and in addition, one contains a minor amount of hematite and 3 contain jarosite. In all samples the band near 0.9 μm is much more weakly expressed than for most samples in the previous four figures (5-8), and the exact position of the minimum, which is difficult to determine precisely with such a broad shallow band, varies.

In general, the position of the band near 0.9 μm is a reliable indicator of the dominant ferric iron-bearing mineral present. If the band is centered distinctly toward wavelengths shorter than 0.9 μm, the dominant iron-bearing mineral is generally hematite. If the band is centered at or above 0.9 μm, the dominant mineral is usually goethite or jarosite. The relative importance of jarosite can be assessed by the presence of the diagnostic sharp 0.43 μm absorption band. Strength of the 0.9 μm absorption and amount of dropoff toward 0.35 μm are related to the total concentration of iron-bearing minerals present. Iron mineral percentages must be determined optically, however, and are not available for precisely the same material as that examined with the spectrophotometer. Thus, quantitative comparison of iron mineral percentage and strength of spectral bands is not possible with the presently available data.

Vibrational Processes

The spectra from 0.35 to 2.5 μm of the particulate rock samples are grouped according to alteration type and are displayed in figures 10 through 15. In each of these figures, the spectra are arranged according to similarity of the features they show at wavelengths longer than 1.3 μm. The spectra are displaced vertically for ease of comparison, and at wavelengths shorter than 1.3 μm the curves are allowed to overlap where necessary because the features in that region have already been discussed.

All the bands that appear at wavelengths longer than 1.3 μm are caused by vibrational processes that occur in the hydroxyl-bearing

minerals that the rock contains, and quite typically the features of just one of these minerals will dominate the spectrum. Features in individual rocks will be discussed under the heading of the alteration type to which each rock belongs.

Silicified Rocks

The spectra of the 34 silicified rock samples are shown in figures 10 and 11. Almost all samples (30) contain alunite, and it is a major constituent in 24, and consequently alunite features dominate many of the spectra. The other feature-producing minerals in order of frequency of occurrence in the rocks, are kaolinite (in 10); jarosite (in 11); gypsum (in 5); and pyrophyllite (in 3). In most spectra, multiple features occur near 1.4 and 2.2 μm. In many, a single band near 1.75 μm is obvious, and in more than half the "water" band near 1.9 μm is apparent.

Twelve rock spectra are assembled in figure 10. These spectra show variations in the position and detailed structure of the bands, and are arranged to emphasize the gradual progression of the 1.4 μm features toward longer wavelengths and to illustrate that the most concentrated mineral does not necessarily produce the most intense features in particulate rock samples, although this is typically the case.

With the exception of the top sample, 81-8-4, all of the samples whose spectra appear in figure 10 contain alunite, in quantities ranging from 1 to about 20 percent, and seven samples also contain kaolinite. Kaolinite is the most abundant hydroxyl-bearing mineral present in the rock designated 81-8-4, and its spectrum, shown at the top of figure 10, is very similar to that of pure kaolinite. It is also very similar in

appearance to the spectrum immediately below it, 100-4-1, which is of a sample containing more than 10 percent of both kaolinite and alunite, with kaolinite more abundant than alunite. The spectrum is dominated by kaolinite, and the only indication of the presence of alunite is a very weakly expressed band that appears near 1.75 μm.

The next spectrum below this, that of sample 109-7-2, which contains comparable amounts of alunite, pyrophyllite, and kaolinite, reflects the presence of the pyrophyllite and kaolinite more intensely than of the alunite, with the single intense features of pyrophyllite at 1.4 and 2.2 μm being quite apparent.

The next three lower spectra, 109-2-7, 109-4-1, and 109-4-4, are of samples that contain significant quantities of kaolinite: between about 10 and 20 percent; they also contain a range of alunite concentrations--minor in 109-2-7--but about the same amount as kaolinite in 109-4-1 and 109-4-4. In all three spectra, the kaolinite doublet near 1.4 μm is apparent, and in the lower two, the longer wavelength member of the alunite doublet is apparent and its intensity reflects the alunite concentration. These two samples also contain minor quantities of gypsum which contribute quite strongly to the 1.9 μm "water" band as well as intensifying the 1.75 μm feature.

The next lower spectrum, 81-4-7, reflects the presence of opal in the rock, and it is this mineral which is primarily responsible for the broadened appearance of the 1.4 and 1.9 μm bands, to which contributions are also made by the minor alunite which produces the bands near 2.2 μm.

The next lower three spectra, 45-11-10, L-15, and 23-2-4, are of

samples that contain alunite (between about 5 and 15 percent), as well as potassium mica in the lower two. The mixture of spectral features is consistent with these compositions, the 1.9 μm water feature being relatively well pronounced when potassium mica is present.

Sample J8-19, which contains alunite, kaolinite, pyrophyllite, and jarosite, produces a fairly broadened spectrum in which the jarosite is largely responsible for the enhanced intensity of the feature near 1.5 μm.

The bottom spectrum (81-8-6) in figure 10 is essentially identical with that of alunite, and indeed, alunite composes more than 20 percent of the rock and is the only hydroxyl-bearing mineral present. It is included here for comparison with the above spectra. Its spectrum is repeated at the top of figure 11, which also displays the spectra of the 23 other silicified rock samples.

With the exception of the lowest six, the spectra shown in figure 11 are very similar, the only obvious differences between them being the presence or absence of the "water" band near 1.9 μm. All display features typical of alunite, and indeed, alunite is present in all of them in quantities ranging from about 10 to 40 percent, with most containing near 20 percent. The appearance of the 1.9 μm band in the lower part of the group can be attributed to the presence of traces of adsorbed water, or where the band is particularly well prounced, such as in L-12, it is due to the presence of potassium mica (10 percent), or in samples 45-11-11, 45-11-12, and 45-11-15, to the presence of minor gypsum.

In the lowest six spectra the features are not well pronounced. The top two, 23-1-14 and 23-1-13, both contain alunite and jarosite but their features are not well-resolved. 82-2-2 contains about 1 percent kaolinite, while the lowest three spectra are of samples in which petrographic analysis failed to detect any clay minerals or alunite, and their spectra indicate by the poorly expressed 1.4 and 1.9 μm bands only the presence of small quantities of water.

Advanced Argillic

Figure 12 shows the spectra of 21 rock samples that display advanced argillic alteration. In this particular figure, bands that are due to a specific mineral are indicated by vertical lines.

The top spectrum (T4-11) owes its overall shape almost entirely to the presence of about 30 percent diaspore with the sharp bands near 1.4 and 2.2 μm being enhanced by the presence of about 5 percent pyrophyllite. The pyrophyllite features are indicated in the next two spectra immediately below (T4-10, T4-13) which are of rocks containing about 50 percent and 70 percent pyrophyllite, with roughly 5 percent diaspore present contributing to the downward slope from 1.5 μm to longer wagelengths.

The three spectra below these, CS-1-2, CS-1-15, CS-1-11, also display the well-resolved features due to the pyrophyllite present (about 5 to 15 percent), and as well display sharp bands adjacent to them due to the presence of larger quantities of potassium mica. That there is more than one mineral (here potassium mica and pyrophyllite) contributing to each of these spectra is evidenced by the structure of the

doubled bands near 1.4 μm, in which the shorter wavelength feature is the more intense. In individual phyllosilicate minerals, when doublets occur near 1.4 μm, the longer wavelength band is typically the more intense. This behavior is apparent in the next five spectra, which are of rocks in which kaolinite is the major constituent, being present in concentrations greater than 30 percent, and the positions of the features due to kaolinite are indicated. In these spectra, the asymmetrical band centered near 1.9 μm is completely characteristic of the presence of molecular water. The petrographic analyses do not indicate the presence of any specific minerals bearing constitutional water (such as gypsum or montmorillonite), but water is frequently associated with clay minerals as physiadsorbed water. In all five of these samples minor, but significant, quantities of alunite are indicated to be present (ranging from about 3 to more than 10 percent) and this is probably responsible for causing the appearance of the weak feature at just longer wavelengths than the very sharp features near 1.4 μm.

The ten spectra shown at the bottom of figure 12 all display the six characteristic features of alunite, starting with the doublet near 1.4 μm, the very diagnostic 1.75 μm feature (which is only present in some other sulphates, such as gypsum) which should prove particularly useful for remote-sensing purposes, the intense feature near 2.17 μm with its supplementary band at slightly longer wavelengths, and the quite well-defined, but typically much weaker, feature near 2.3 μm. These ten samples contain between about 25 and 50 percent alunite, which is completely consistent with their spectra. Two of the samples,

45-11-20 and 81-8-3, also display weak 1.9 μm "water" bands. They are the only two samples in this group that petrographic analysis indicates also contain significant, although minor, amounts of kaolinite (samples 81-4-1 and 23-1-5 contain only traces of kaolinite).

Advanced Phyllic and Phyllic

The top six curves in figure 13, which all display a well-defined 0.85 μm minimum, are the spectra of rocks having advanced phyllic alteration, while the bottom ten spectra are those of rocks having phyllic alteration.

All the samples displaying advanced phyllic alteration contain potassium mica (about 3 to 45 percent), and, with the exception of CS-1-7, also contain large quantities of alunite (about 10 to 45 percent). It is the bands due to these minerals that dominate the spectra, as evidenced by multiple bands near 1.4 and 2.2 μm, to which both minerals contribute in various proportions as well as to the well-defined band at 1.75 μm characteristic of alunite and the 1.9 μm feature attributable to water associated with the potassium mica and opal. This 1.9 μm water band is particularly pronounced in the spectrum of sample J8-3 (shown fifth from the top of figure 13) which consists of about 35-40 percent potassium mica and 30 percent opal.

The top spectrum (CS-1-7) is dominated by the features of potassium mica (~45 percent) alone, there being only ~1 percent alunite present, so small an amount that the 1.75 μm band is not observable.

The lower ten spectra are all of phyllic-altered rocks. With the exception of the top spectrum (J8-8), they do not display an intense 0.85 μm minimum and all are relatively flat with weak but quite well-

defined 1.4, 1.9, and 2.2 μm features. All contain large quantities of potassium mica (10 to 50 percent) with little or no kaolinte (~3 percent at most).

The spectrum shown at the bottom of figure 13, sample CP-1-12, shows none of the features expected from a rock composed of more than 50 percent potassium mica with minor kaolinite. Its maximum reflectivity is only about 50 percent that of any of the other samples, suggesting the presence of some material that drastically lowers reflectivity and masks well-resolved bands in the near-visible infrared region. The most likely possibility is magnetite or another similar iron spinel, but no such mineral was definitely identified, and maximum concentration could be no more than about 5 percent

Montmorillonitic-Argillic Rocks

The rock samples displaying this type of alteration contain between 25 and 55 percent montmorillonite, and with one exception (CP-1-13), their spectra, shown in figure 14, are dominated by the intense single hydroxyl and water vibrational bands that occur near 1.4, 1.9, and 2.2 μm.

The spectra 109-2-8, 109-2-5, and 109-2-3, are essentially identical to that of montmorillonite, displaying only single features, which indicates that any contributions from the small percentages of kaolinite (<5 percent) present only tend to emphasize those features due to the montmorillonite.

The three spectra above those (24-4-3, 24-4-8, and 24-4-10) display multiple features, especially near 1.4 and 2.2 μm, due to the presence

of minor amounts of alunite, which is not abundant enough to produce more than the suggestion of a band at 1.75 μm. In the lowest of these three spectra (24-4-3) the 2.2 μm feature is broadened, because this sample also contains a significant quantity (~15 percent) of gypsum.

The topmost spectrum is of a sample (45-11-19) that does not contain alunite, but does contain ~10 percent jarosite, and it is this that produces the supplementary bands near 1.4 and 2.2 μm.

The lowest spectrum, that of CP-1-13, even though the rock contains more than 50 percent montmorillonite, does not display any well-defined bands. Like sample CP-1-12, whose spectrum is shown in figure 13 for phyllic rocks, its low reflectivity and lack of features may be caused by the suppressing effects of the presence of magnetite.

Miscellaneous Alteration Types

Of the eight spectra shown in figure 15, the top six all show numerous well-defined bands, including the 1.9 μm "water" band, and they are of rocks in which opal is the most abundant constituent.

It is the presence of the large amounts of opal in these samples that accounts wholly or mainly for the appearance of the water band. The two top spectra, 221-1-8 and 221-1-6, display all the features of alunite and these samples each contain 15 to 20 percent alunite. The additional small sharp band on the short wavelength side of the 1.4 μm group in 221-1-6 is due to the presence of kaolinite in that sample.

The next lower two spectra (24-5-9, 24-5-10) are essentially identical to each other. The samples each contain 10-15 percent alunite which accounts for the bands characteristic of it, but additional fea-

tures are obvious, particularly the well-resolved doublet which partly obscures the shortest wavelength feature of the alunite. The doublet is characteristic of the presence of kaolinite, which the samples also contain in amounts of 10-15 percent.

In the next lower two spectra, the kaolinite features are clearly intensified, as in the 1.75 μm band and the 1.9 μm feature, particularly in the upper spectrum, 24-5-6. These samples also contain 10-15 percent of both kaolinite and alunite, but in addition, they contain gypsum to the extent of about 15 percent in 24-5-6 and 2 percent in 24-5-4. It is the constitutional water in gypsum which accounts for the very pronounced 1.9 μm feature and which intensifies the 1.75 μm band in 24-5-6. Gypsum, like alunite, is also a sulphate and it is the only other common mineral in these rocks that produces a band near 1.75 μm. Because the amount of gypsum is much less in 24-5-4, these two features are less pronounced but the 1.9 μm feature is considerably broadened and less deep.

The spectrum of sample 4-29-5, a rhyolitic ash flow, contains ~50 percent montmorillonite, which produces the 1.4 and 1.9 μm features, and the weak features near 2.2 μm.

Spectrum 08-09-08 is that of a quartz-sericite rock with features attributable to the presence of water and potassium mica (2.2 μm). It is similar in mineralogy and spectral features to the phyllic rocks described above (see fig. 13).

CONCLUSIONS

The particulate samples of the hydrothermally altered rocks studied here typically display clearly defined bands in their bidirectional reflection spectra caused by absorptions due to both electronic and vibrational processes. Between 0.35 and 1.3 μm, electronic transitions in the iron-bearing minerals, hematite, goethite, montmorillonite, and jarosite cause characteristic features, in the form of minima, to occur near 0.43, 0.65, 0.85, and 0.93 μm. In the range from 1.3 to 2.5 μm the characteristic minima are caused by vibrational transitions in a number of constituent clay, sulfate, and water-bearing minerals, namely: alunite, kaolinite, montmorillonite, pyrophyllite, potassium micas, diaspore, gypsum, and jarosite, and carbonates. Bands due to these latter minerals are concentrated in quite narrow spectral regions near 1.4, 1.75, 1.9, 2.12, and 2.35 μm.

Certain generalizations can be made concerning the appearance of the individual spectral features in these hydrothermally altered rocks:

a) The appearance of a very sharp but weak band near 0.43 μm appears to be completely diagnostic of the presence of jarosite;

b) The presence of hematite as a major constituent produces a broad intense minimum centered near 0.85 μm;

c) The presence of goethite as a major constituent produces a similar feature centered near 0.93 μm;

d) When both hematite and goethite are present in significant proportions, the combination of these two features produces a band with its minimum between 0.85 and 0.93 μm;

e) The development of a supplementary band which appears as a short wavelength shoulder on the 0.75 μm maximum, and centered near 0.65 μm is typically more pronounced for goethite-rich samples than for hematite-rich samples;

f) The presence of clay minerals and alunite is indicated by bands near both 1.4 and 2.2 μm;

g) The presence of pyrophyllite or potassium micas is indicated by intense, sharp, single minima near 1.4 and 2.2 μm;

h) Clearly doubled sharp features near both 1.4 and 2.2 μm, of which the shorter wavelength member in both groups of bands is the less intense, indicates the presence of kaolinite;

i) The presence of alunite is also indicated by the appearance of doubled features near 1.4 and 2.2 μm, but in this case, in the doublet near 2.2 μm, it is the longer wavelength member that is less intense; and, in addition, a very diagnostic minimum appears near 1.75 μm as well as a sharp feature near 2.3 μm;

j) The presence of montmorillonite is indicated, in addition to broad 1.4 and 2.2 μm features, by the appearance of an intense 1.9 μm "water" band. This latter band very often appears weakly when opal or potassium mica is present, and sometimes when kaolinite is present;

k) When gypsum is present, features similar though somewhat broader than those displayed by montmorillonite appear, but, in addition, a feature near 1.75 μm, similar to that in alunite, also occurs, as it also sometimes does when large amounts of jarosite are present;

1) The presence of diaspore imparts an unusual shape to the rock spectrum, causing the intensity of the spectrum to drop quite sharply from 1.5 to 1.9 μm, similar to the spectrum of pure diaspore.

On the basis of the rock samples investigated here, some observations about the different types of alteration can be made:

a) Almost all spectra show intense 1.4 and 2.2 μm minima;

b) With just a few exceptions, all the spectra display a rapid decrease in reflectivity from 1.4 μm to shorter wavelengths, with the reflectivity at 0.35 μm being the minimum value. The exception to this general behavior is for the phyllic rocks, which typically begin their descent from near 0.7 μm;

c) The advanced argillic rocks show by far the best resolved and most intense vibrational features, and as a class they are closely followed by the silicified samples in this respect;

d) The only alteration samples that show unique features as a class are the montmorillonitic argillic rocks, for which all (with one exception) display spectra that are essentially identical with that of pure montmorillonite;

e) The phyllic rocks are also quite distinct (again with one exception) in that their spectra are quite flat from 0.7 to 2.5 μm and show very weakly expressed iron bands near 0.9 μm and very weak 1.4, 1.9, and 2.2 μm features;

f) The spectra of the advanced phyllic samples are dominated by the features of alunite, together with a well-defined 1.9 μm "water" band due to potassium mica and opal. Half of the silicified rock spectra

are indistinguishable from a pure alunite spectrum as far as the positions and relative intensities of the bands are concerned, and lack the 1.9 μm "water" feature. The rest of the advanced argillic samples, which do not contain major amounts of alunite, display well-defined and clearly identifiable features of other minerals they contain, and this, to a lesser extent, is true for the rest of the silicified samples and many of the opalized samples;

g) Because alunite occurs as a major constituent in so many of this suite of hydrothermally altered rock samples, and because the alunite spectrum appears to be so dominant, it would be difficult to classify a sample into an alteration type on the basis of its spectrum alone. When alunite is absent, the task becomes much easier. However, the four alteration types that contain alunite (silicified, advanced argillic, advanced phyllic, and opalized) are usually not all present in a single hydrothermally altered area, and those that are present tend to form contiguous zones;

h) Comparison of the spectral data with that obtained from petrographic and X-ray analyses reveals that the detection and identification of a mineral in the rocks by spectroscopic techniques is confirmed by the other techniques. However, certain minerals were detected less frequently in these spectra than by other techniques, and this was usually because the features of one mineral spectrum will dominate and mask those of a less concentrated constituent.

Nevertheless, the potential of spectroscopy to detect and confirm the presence of clay minerals in altered rocks is clearly indicated,

and its usefulness as a very rapid and reliable analytical tool is demonstrated. For example, the mere appearance of the 2.2 μm feature indicates the presence of an hydroxyl-bearing mineral, and, in combination with a feature at 1.75 μm and the absence of a 1.9 μm band, is completely diagnostic of alunite. The potential for making this a quantitative technique is obvious, and the availability of the 1.5 to 2.5 μm region (with the exception of the 1.9 μm region) points up the potential importance of this type of data for remote-sensing purposes.

REFERENCES

Abrams, M. J., Ashley, R. P., Rowan, L. C., Goetz, A. F. H., and Kahle, A. B., 1977, Mapping of hydrothermal alteration in the Cuprite mining district, Nevada, using aircraft scanner images for the spectral region 0.46 to 2.36 μm: Geology, v. 5, p. 713-718.

Hunt, G. R., and Ross, H. P., 1967, A bidirectional reflectance accessory for spectroscopic measurements: Applied Optics, v. 6, p. 1687-1890.

Hunt, G. R., and Salisbury, J. W., 1970, Visible and near-infrared spectra of minerals and rocks--I. Silicate minerals: Modern Geology, v. 1, p. 283-300.

_____1971, Visible and near-infrared spectra of minerals and rocks--II. Carbonates: Modern Geology, v. 2, p. 23-30.

Hunt, G. R., Salisbury, J. W., and Lenhoff, C. J., 1971a, Visible and near-infrared spectra of minerals and rocks--III. Oxides and hydroxides: Modern Geology, v. 2, p. 195-205.

_____1971b, Visible and near-infrared spectra of minerals and rocks--IV. Sulphides and sulphates: Modern Geology, v. 3, p. 1-14.

_____1973, Visible and near-infrared spectra of minerals and rocks--VI. Additional silicates: Modern Geology, v. 4, p. 85-106.

Manning, P. G., 1973, Extinction coefficients of Fe^{3+} spectral bands as indicators of local crystal compositions: Canadian Mineralogist, v. 12, p. 120-123.

Meyer, Charles, and Hemley, J. J., 1967, Wall rock alteration, Chapter 6, in Barnes, H. L., ed., Geochemistry of hydrothermal ore deposits: New York, Holt, Rinehart, and Winston, Inc., 670 p.

Rossman, G. R., 1976, Spectroscopic and magnetic studies of ferric iron hydroxy sulphates--The sines $Fe(OH)SO_4 \cdot NH_2O$ and the jarosites: American Mineralogist, v. 61, p. 398-404.

Rowan, L. C., Wetlaufer, P. H., Goetz, A. F. H., Billingsley, F. C., and Steward, J. H., 1974, Discrimination of rock types and detection of hydrothermally altered areas in south-central Nevada by the use of computer-enhanced ERTS images: U.S. Geological Survey Professional Paper 883, 35 p.

Rowan, L. C., Goetz, A. F. H., and Ashley, R. P., 1977, Discrimination of hydrothermally altered and unaltered rocks in visible and near-infrared multispectral images: Geophysics, v. 42, p. 522-535.

Tatlock, D. B., 1966, Rapid modal analysis of some felsic rocks from calibrated X-ray diffraction patterns: U.S. Geological Survey Belletin 1209, 41 p.

Table 1.--Sample Series Identification and Localities in Western Nevada

Sample series	Locality	Quadrangle map name	Section, Township, Range
J8-	Goldfield mining district	Goldfield	Sec. 10, T. 3 S., R. 43 E.
T4-	Goldfield mining district	Goldfield	Sec. 5, T. 3 S., R. 42 E.
L-	Goldfield mining district	Goldfield	Sec. 7, T. 3 S., R. 42 E.
23-	Goldfield mining district	Goldfield	Secs. 9, 10, T. 3 S., R. 43 E.
45-	Goldfield mining district	Goldfield	Sec. 12, T. 3 S., R. 43 E.
24-	Goldfield mining district	Goldfield	Sec. 34, T. 2 S., R. 43 E.
4-29-	Goldfield mining district	Goldfield	Sec. 2, T. 4 S., R. 42 E.
5-3-	Goldfield mining district	Goldfield	Sec. 34, T. 3 S., R. 44 E.
221-1-	Cuprite mining district	Goldfield	Sec. 5, T. 5 S., R. 42 E.
109-	Geiger Grade altered area	Virginia City	Sec. 26, T. 18 N., R. 20 E.
81-	Geiger Grade altered area	Virginia City	Sec. 35, T. 18 N., R. 20 E.
100-	Washington Hill	Virginia City	Secs. 27, 33, 34, T. 19 N., R. 21 E.
08-09-	Rock Hill mining district	Rock Hill	Sec. 34, T. 4 N., R. 36 E.
CP-1-	Castle Peak mine, Gilbert mining district	Devil's Gate	Unsurveyed
CS-	Cactus Springs mining district	Cactus Springs	Sec. 12, T. 3 S., R. 45 E.
5-2	Cow Camp Spring	Lida Wash	Sec. 34, T. 3 S., R. 38 E.

Table 2.--Abbreviations Assigned to Minerals and Used in Figures

Ab	Albite	G	Goethite*	M	Montmorillonite*
Al	Alunite*	Gyp	Gypsum*	Op	Opal
B	Biotite*	Ha	Halite	Opaq	Opaque
Ba	Barite	Hem	Hematite*	P	Plagioclase
Br	Brookite	J	Jarosite*	Pp	Pyrophyllite*
Ca	Calcite*	K	Kaolinite*	Q	Quartz
Chl	Chlorite*	Km	K-mica*	Rt	Rutile
D	Diaspore	Kf	K-feldspar	Zl	Zeolite*
Ep	Epidote*	Lx	Leucoxene		

* Minerals that produce well-defined spectral features in the 0.35 to 2.5 μm range.

Table 3.--Major Minerals Present in Rocks Studied and Content Criteria for Alteration Types

Alteration Type	Major Minerals*	Criteria
Silicified	Q±Al±K±Pp±D±Km	Vol. % quartz > w+% SiO_2 of original rock
Advanced argillic	Q±Al±Pp±K±D±Op±Km	Must contain kaolinite or pyrophyllite, and alunite
Opal	Op±Q±K±Pp±Al±D±Km	Opal > quartz
Advanced phyllic	Q±Al±Km±Op	Must contain alunite and K-mica; kaolinite and pyrophyllite absent
Argillic	Q±K±Km±mixed layer	Must contain kaolinite; kaolinite + mixed-layer clays > K-mica
Phyllic	Q±K±Km±mixed layer	K-mica > clays
Quartz-sericite	A±Km±Kf±Ab	No mixed-layer clays; K-mica probably mostly 2M
Montmorillonite-bearing argillic	M±K±Q±mixed layer ±Ca±Chl	Montmorillonite > calcite; relict plagioclase and K-feldspar common

* See Table 2 for abbreviations.

FIGURE CAPTIONS

Fig. 1. Hydrothermally altered areas sampled in western Nevada.

Fig. 2. Features due to electronic transitions in the spectra of iron-bearing minerals commonly present in hydrothermally altered rocks. Spectra are displaced vertically and characteristic features are indicated by arrows.

Fig. 3. Features due to vibrational processes in the spectra of four hydroxyl-bearing minerals commonly present in hydrothermally altered rocks. Spectra are displaced vertically. Reflection values are indicated on the curves at 1.6 μm.

Fig. 4. Features due to vibrational processes in the spectra of four minerals commonly present in hydrothermally altered rocks. Spectra are displaced vertically. Reflection values are indicated on the curves at 1.6 μm.

Fig. 5. Spectra of rock samples that contain jarosite and display the characteristic ferric iron feature near 0.43 μm (arrows at J). Spectra are displaced vertically and arranged according to alteration type. For sample identification and mineral content code, see tables 1 and 2. Secondary constituents in parentheses.

Fig. 6. Spectra of rock samples that display a minimum near 0.85 μm characteristic of hematitic rocks. Spectra are displaced vertically and arranged according to alteration type. For sample identification and mineral content code, see tables 1 and 2. Secondary constituents in parentheses.

Fig. 7. Spectra of rock samples that contain either hematite or goethite, or both, as minor constituents. All but the lowest 7 display an intense feature between 0.85 and 0.93 μm. In the top spectra the position of the band is governed by the presence of goethite in the sample. The three spectra at the bottom, although containing a significant amount of hematite display no minimum near 0.9 μm. Spectra are displaced vertically. For sample identification and mineral content code, see tables 1 and 2. Secondary constituents in parentheses.

Fig. 8. Spectra of rock samples that display a minimum near 0.93 μm characteristic of the presence of goethite. The lowest two spectra are of samples that do not contain goethite but do contain major jarosite. Spectra are displaced vertically and arranged according to alteration type. For sample identification and mineral content code, see tables 1 and 2. Secondary constituents in parentheses.

Fig. 9. Spectra of rock samples whose mineral analyses did not indicate the presence of iron oxide minerals. Spectra displaced vertically. For sample identification and mineral content code, see tables 1 and 2. Secondary constituents in parentheses.

Fig. 10. 0.35 to 2.5 μm spectra of rock samples classified as silicified, in most of which the features are not primarily determined by the presence of alunite. Spectra are displaced vertically. For sample identification and mineral content code, see tables 1 and 2. Secondary constituents in parentheses.

Fig. 11. 0.35 to 2.5 μm spectra of rock samples classified as silicified, in which the features of most are determined by presence of alunite. Spectra are displaced vertically. For sample identification and mineral content code, see tables 1 and 2. Secondary constituents in parentheses.

Fig. 12. 0.35 to 2.5 μm spectra of rock samples that were classified as displaying advanced argillic alteration. Those vibrational features that are due to the presence of particular constituent minerals are indicated (i.e., Pp = pyrophyllite; Km - potassium mica; K = kaolinite; Al = alunite). Spectra are displaced vertically and arranged according to similarity. For sample identification and mineral content code, see tables 1 and 2. Secondary constituents in parentheses.

Fig. 13. 0.35 to 2.5 μm spectra of rock samples displaying advanced phyllic (top 6 spectra) and phyllic (lower 10 spectra) alteration. Spectra are displaced vertically. For sample identification and mineral content code, see tables 1 and 2. Secondary constituents in parentheses.

Fig. 14. 0.35 to 2.5 μm spectra of rock samples classified as displaying montmorillonitic-argillic alteration. Spectra are displaced vertically. For sample identification and mineral content code, see tables 1 and 2. Secondary constituents in parentheses.

Fig. 15. 0.35 to 2.5 μm spectra of rock samples classified as opalized (top 6 spectra) or which display unusual alteration types (lower 2 spectra). Spectra are displaced vertically. For sample identification and mineral content code, see tables 1 and 2. Secondary constituents in parentheses.

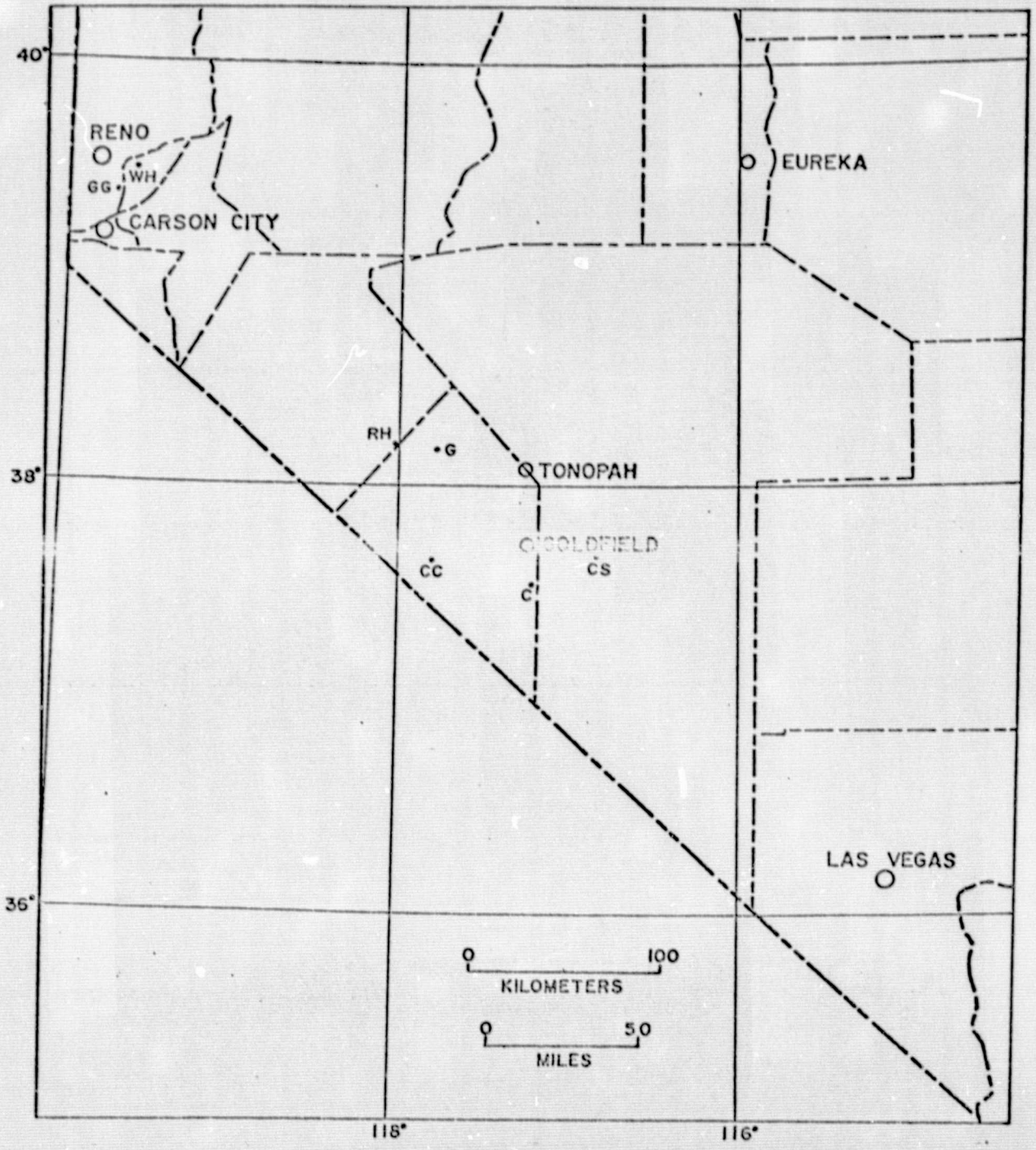

FIG 1

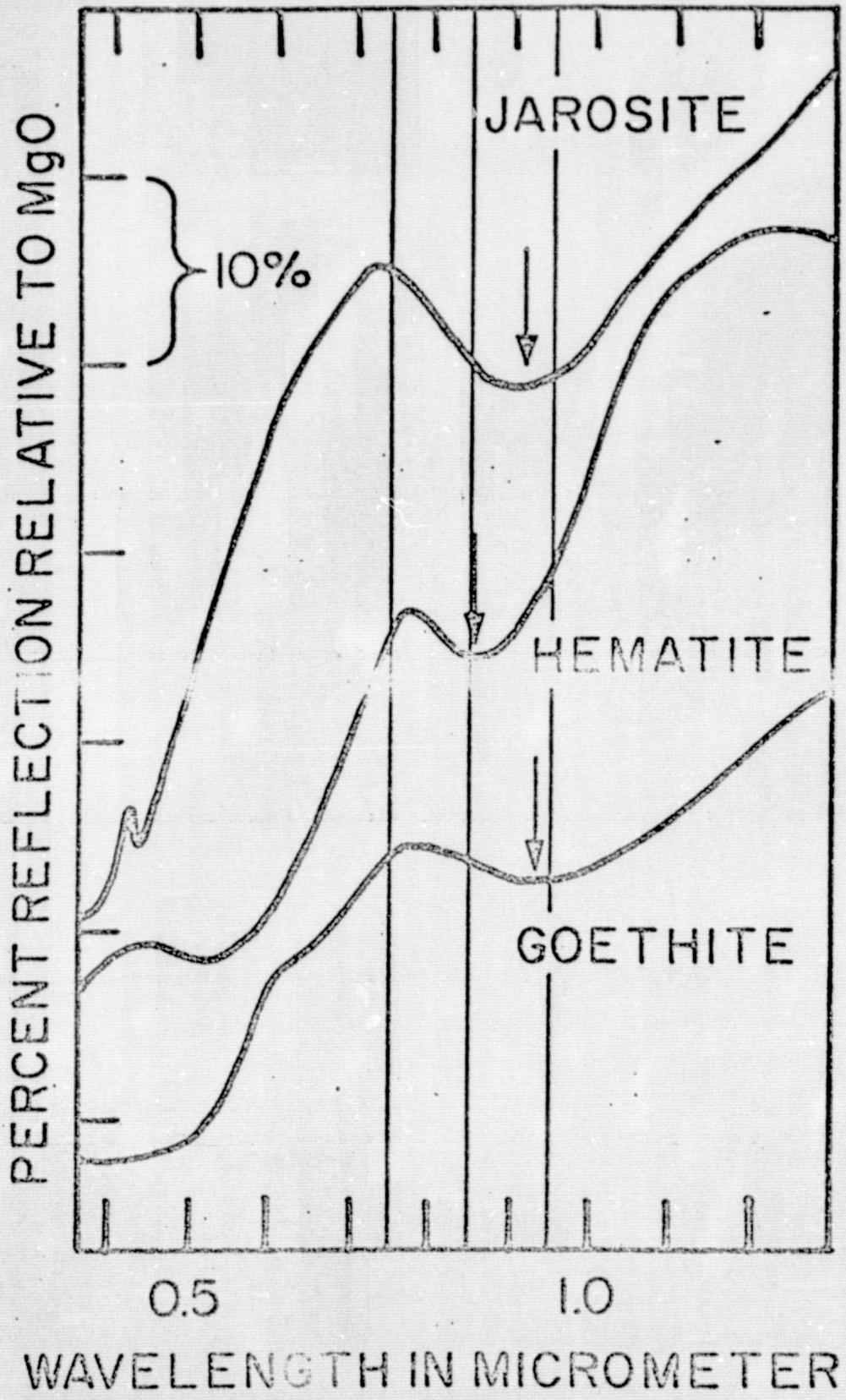
JAROSITE
10%
HEMATITE
GOETHITE
PERCENT REFLECTION RELATIVE TO MgO
0.5
1.0
WAVELENGTH IN MICROMETERS

FIG 2

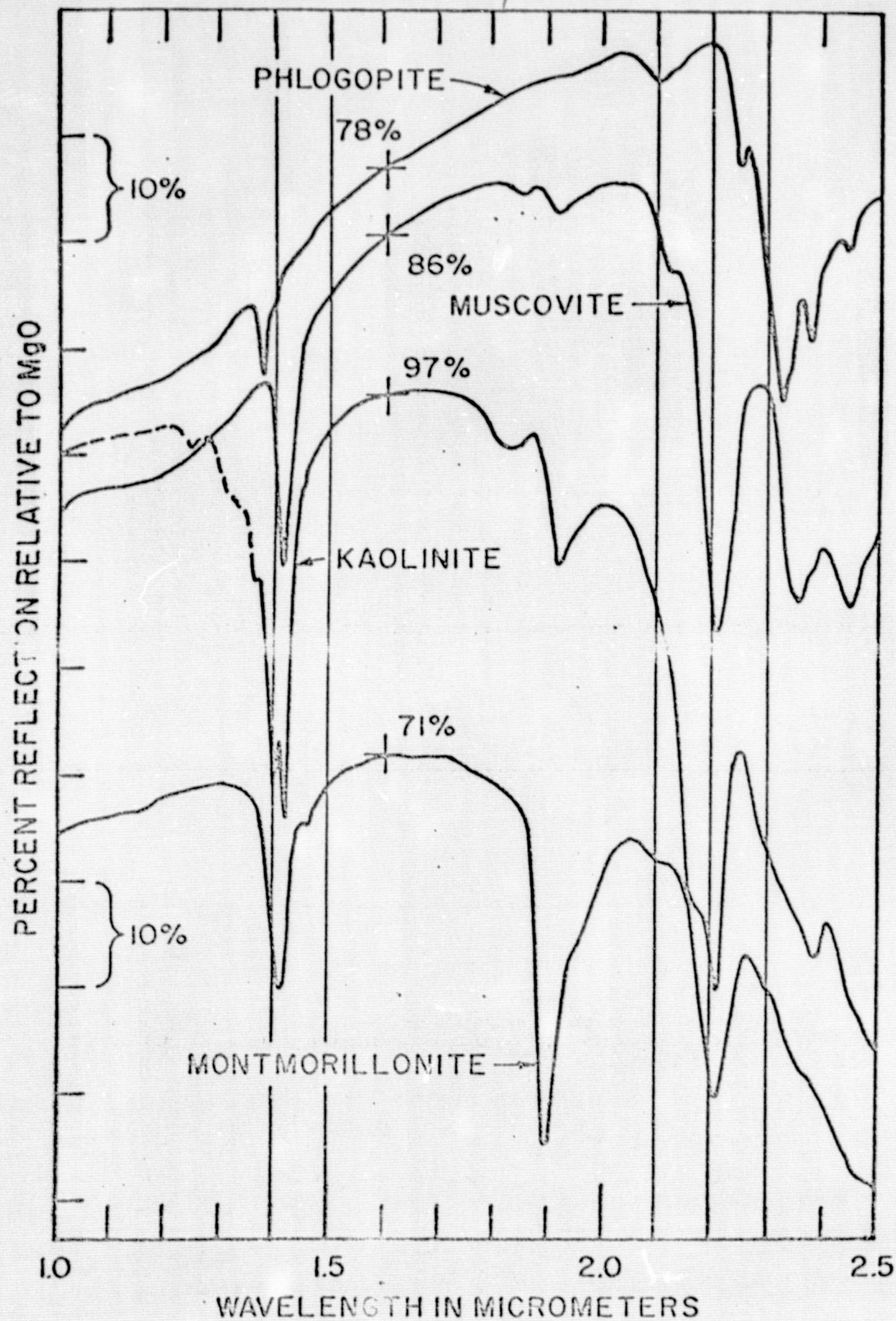

FIG 3

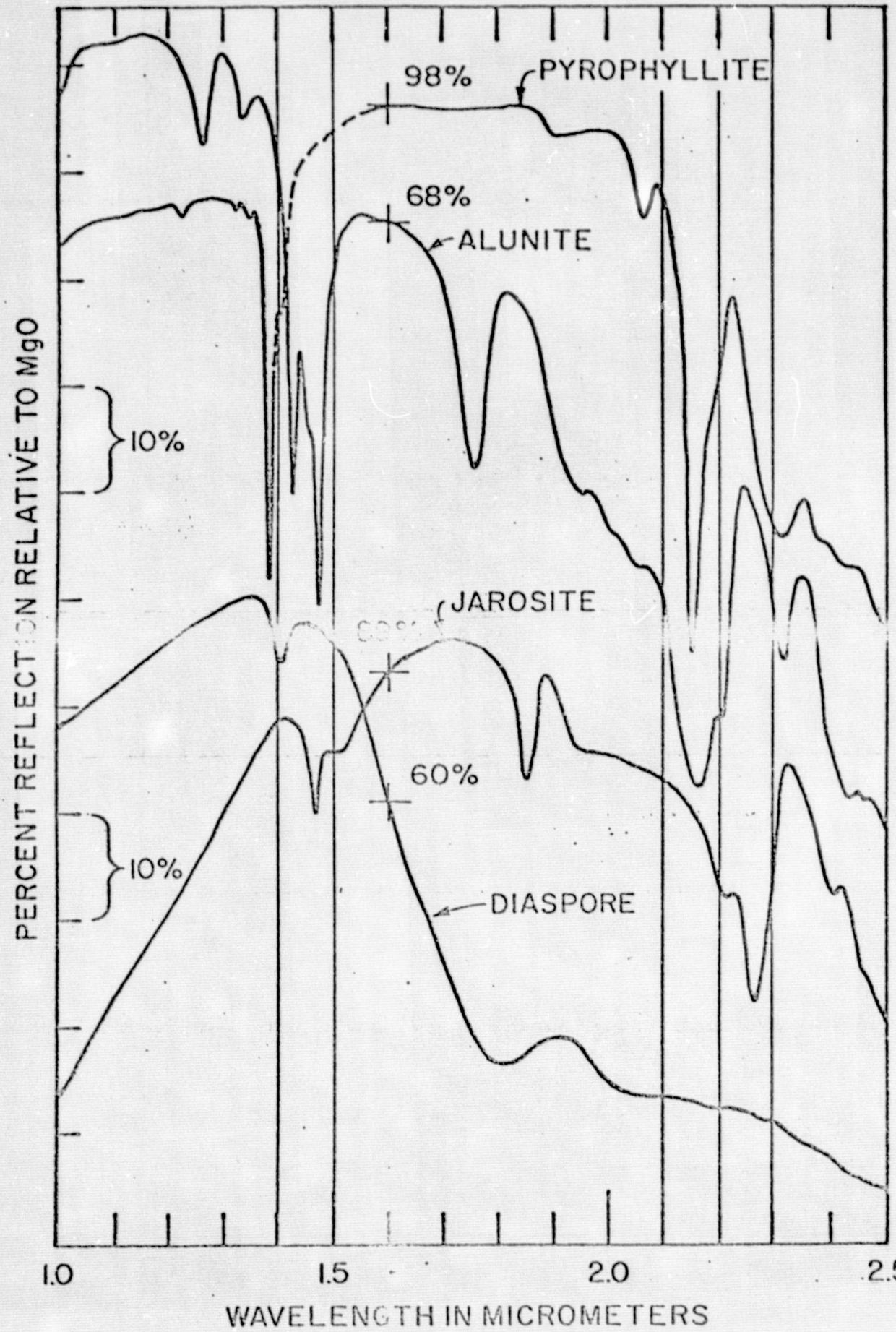
98%
PYROPHYLLITE
68%
ALUNITE
10%
JAROSITE
60%
10%
DIASPORE
PERCENT REFLECTION RELATIVE TO MgO
1.0
1.5
2.0
2.5
WAVELENGTH IN MICROMETERS

FIG 4

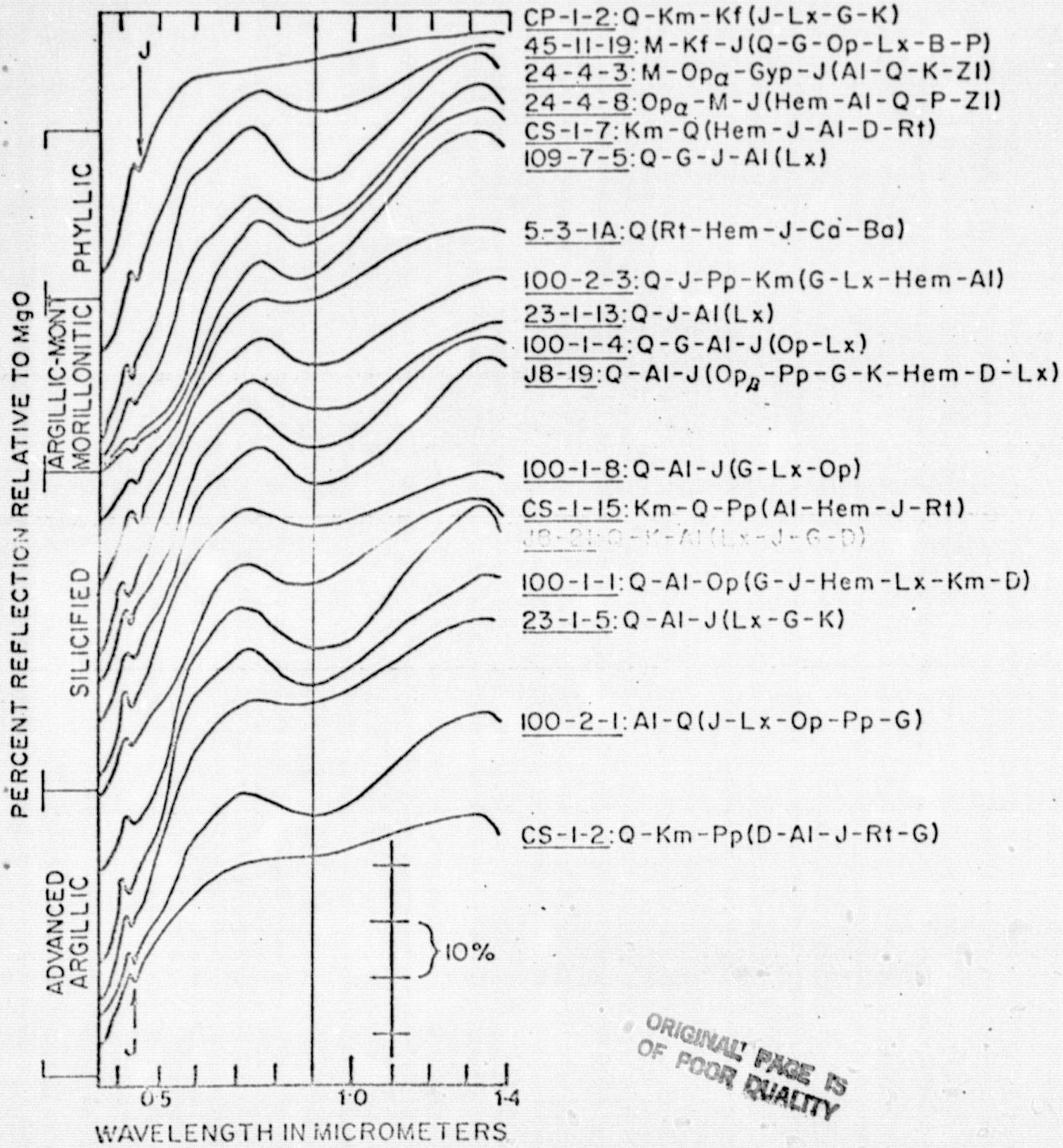

FIG 5

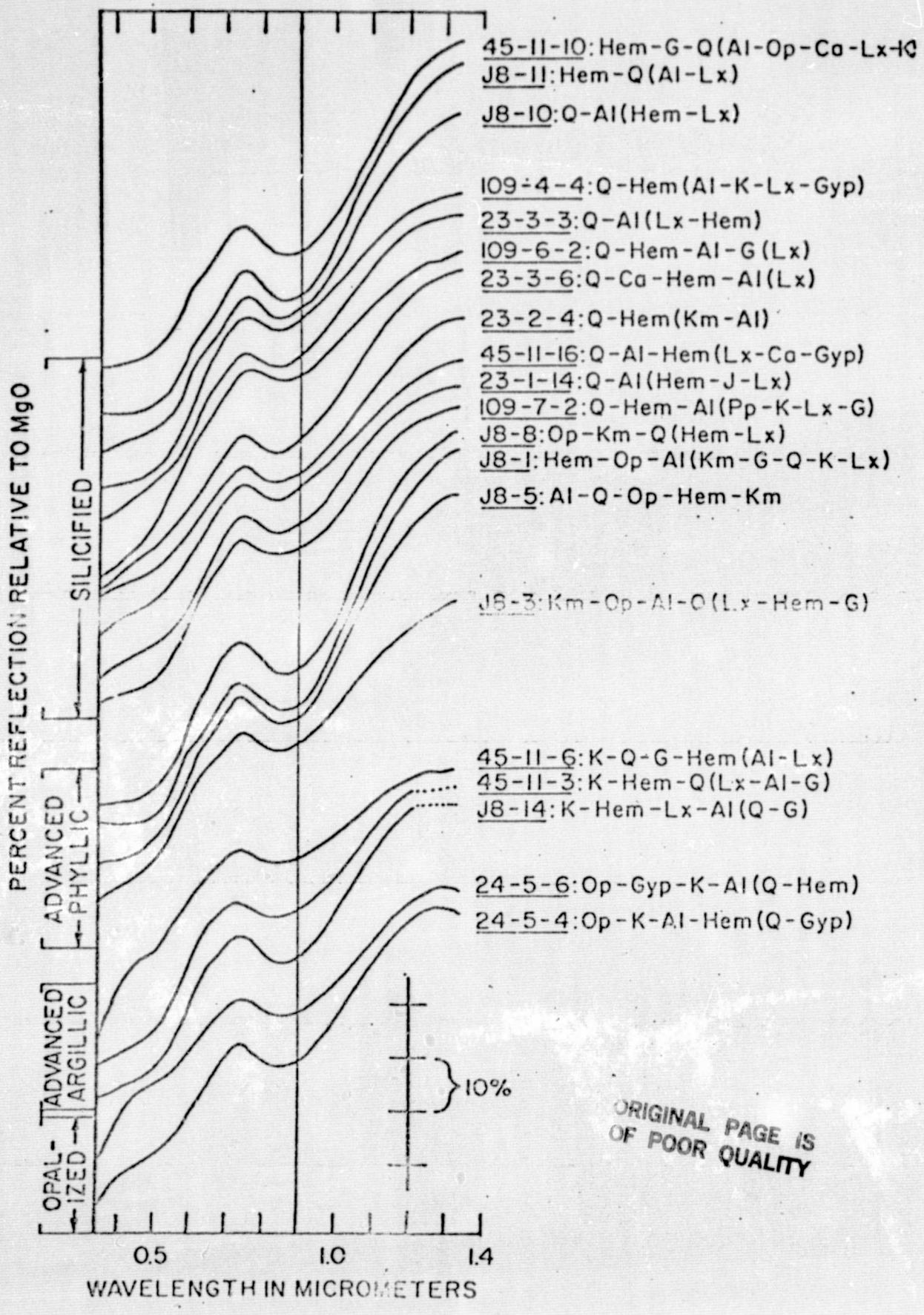

FIG 6

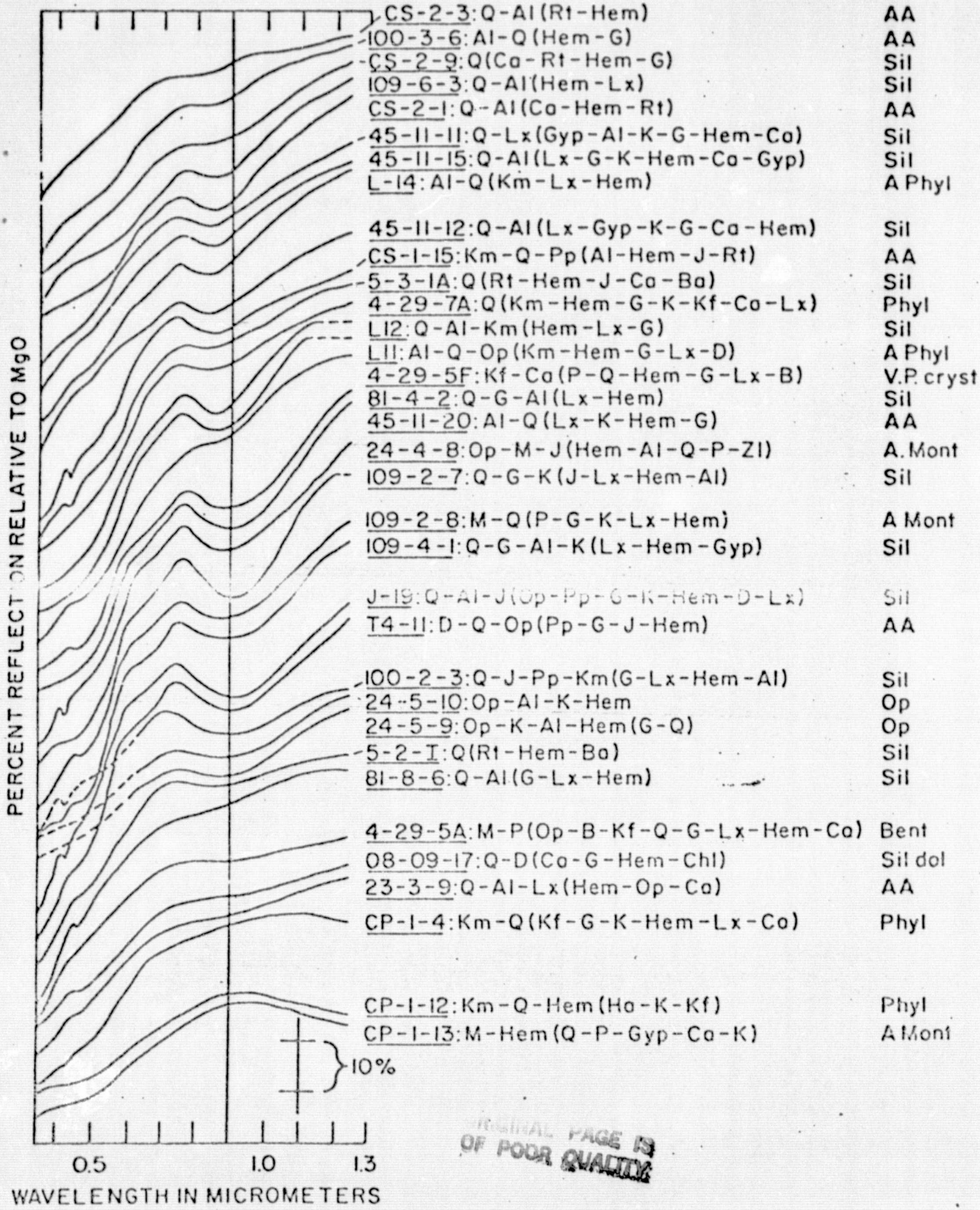

FIG 7

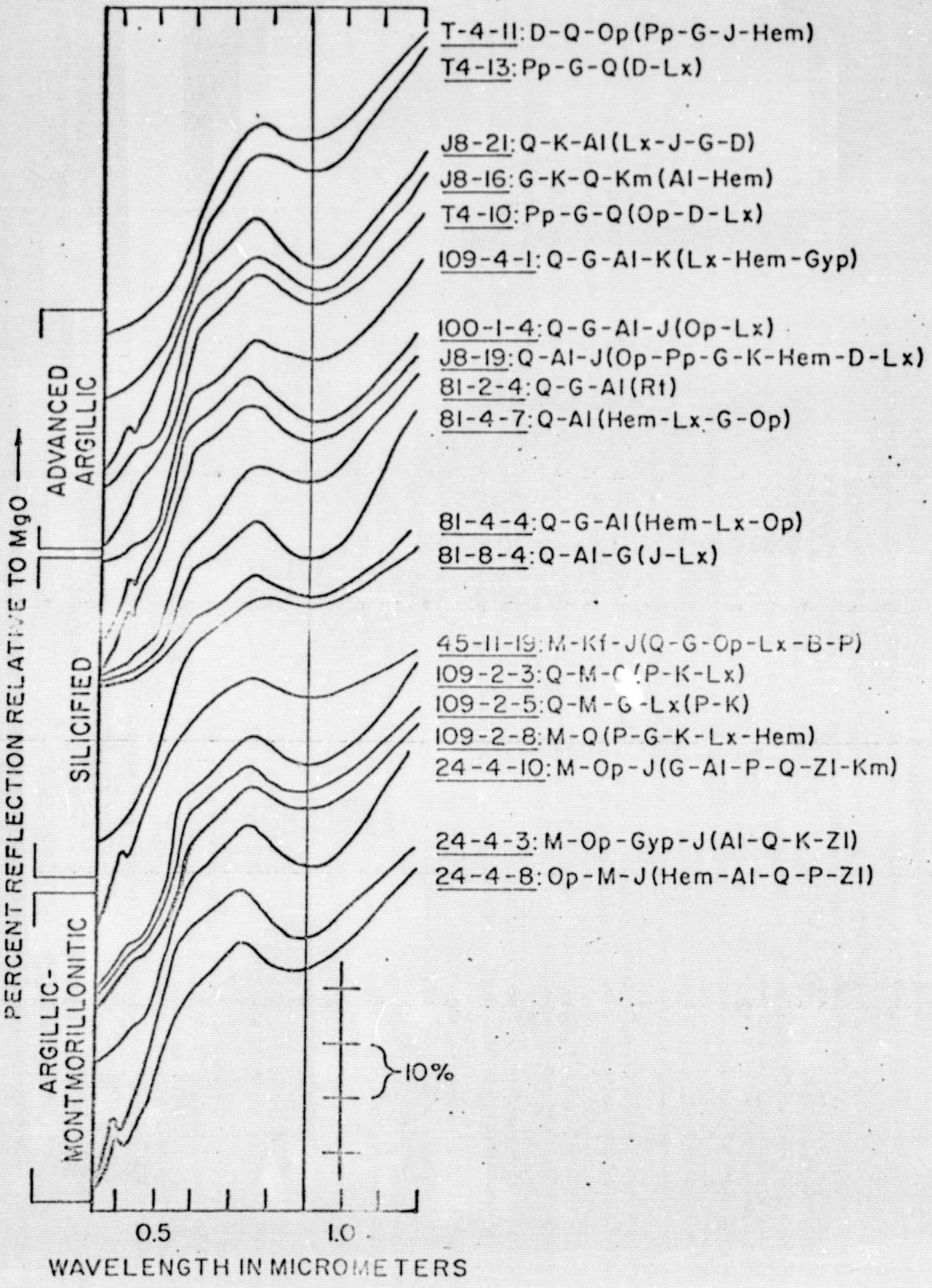
T-4-11: D-Q-Op(Pp-G-J-Hem)
T4-13: Pp-G-Q(D-Lx)
J8-21: Q-K-Al(Lx-J-G-D)
J8-16: G-K-Q-Km(Al-Hem)
T4-10: Pp-G-Q(Op-D-Lx)
109-4-1: Q-G-Al-K(Lx-Hem-Gyp)
100-1-4: Q-G-Al-J(Op-Lx)
J8-19: Q-Al-J(Op-Pp-G-K-Hem-D-Lx)
81-2-4: Q-G-Al(Rt)
81-4-7: Q-Al(Hem-Lx-G-Op)
81-4-4: Q-G-Al(Hem-Lx-Op)
81-8-4: Q-Al-G(J-Lx)
45-11-19: M-Kf-J(Q-G-Op-Lx-B-P)
109-2-3: Q-M-G(P-K-Lx)
109-2-5: Q-M-G-Lx(P-K)
109-2-8: M-Q(P-G-K-Lx-Hem)
24-4-10: M-Op-J(G-Al-P-Q-Zl-Km)
24-4-3: M-Op-Gyp-J(Al-Q-K-Zl)
24-4-8: Op-M-J(Hem-Al-Q-P-Zl)
ADVANCED ARGILLIC
SILICIFIED
ARGILLIC-MONTMORILLONITIC
PERCENT REFLECTION RELATIVE TO MgO
10%
0.5
1.0
WAVELENGTH IN MICROMETERS

FIG 8

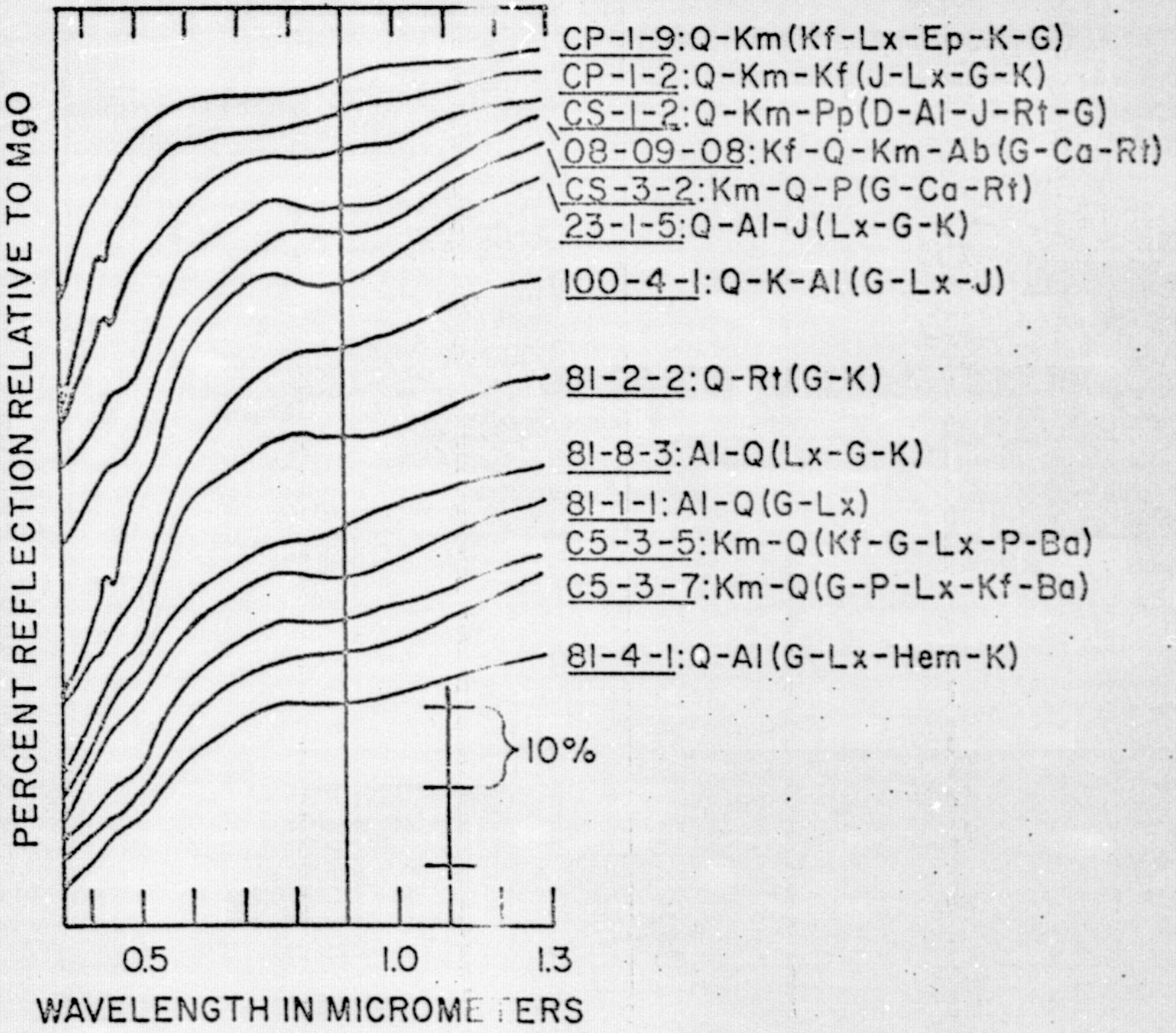
CP-1-9:Q-Km(Kf-Lx-Ep-K-G)
CP-1-2:Q-Km-Kf(J-Lx-G-K)
CS-1-2:Q-Km-Pp(D-Al-J-Rt-G)
08-09-08:Kf-Q-Km-Ab(G-Ca-Rt)
CS-3-2:Km-Q-P(G-Ca-Rt)
23-1-5:Q-Al-J(Lx-G-K)
100-4-1:Q-K-Al(G-Lx-J)
81-2-2:Q-Rt(G-K)
81-8-3:Al-Q(Lx-G-K)
81-1-1:Al-Q(G-Lx)
C5-3-5:Km-Q(Kf-G-Lx-P-Ba)
C5-3-7:Km-Q(G-P-Lx-Kf-Ba)
81-4-1:Q-Al(G-Lx-Hem-K)
10%
PERCENT REFLECTION RELATIVE TO MgO
0.5
1.0
1.3
WAVELENGTH IN MICROMETERS

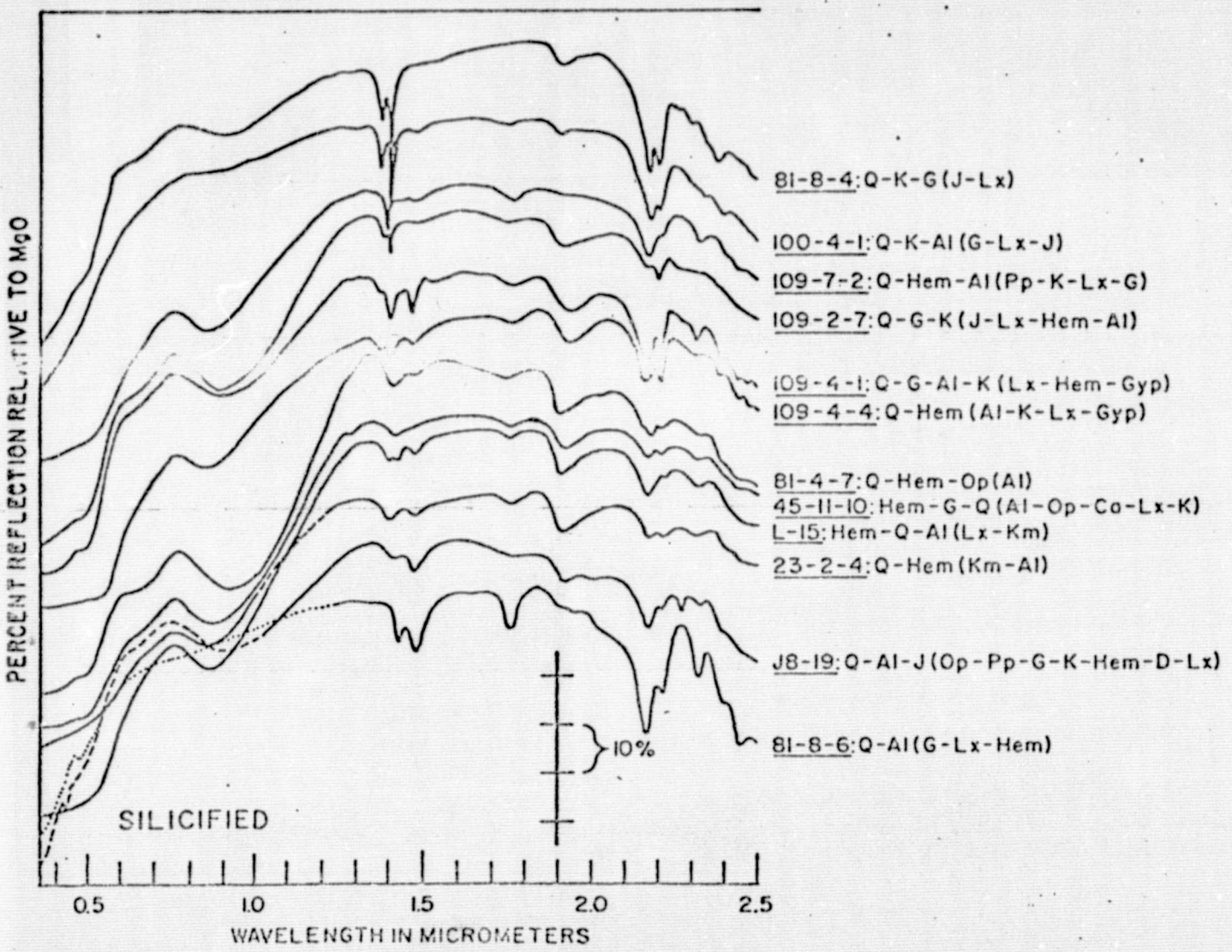
PERCENT REFLECTION RELATIVE TO MgO
81-8-4: Q-K-G (J-Lx)
100-4-1: Q-K-Al (G-Lx-J)
109-7-2: Q-Hem-Al (Pp-K-Lx-G)
109-2-7: Q-G-K (J-Lx-Hem-Al)
109-4-1: Q-G-Al-K (Lx-Hem-Gyp)
109-4-4: Q-Hem (Al-K-Lx-Gyp)
81-4-7: Q-Hem-Op (Al)
45-11-10: Hem-G-Q (Al-Op-Ca-Lx-K)
L-15: Hem-Q-Al (Lx-Km)
23-2-4: Q-Hem (Km-Al)
J8-19: Q-Al-J (Op-Pp-G-K-Hem-D-Lx)
81-8-6: Q-Al (G-Lx-Hem)
10%
SILICIFIED
0.5
1.0
1.5
2.0
2.5
WAVELENGTH IN MICROMETERS

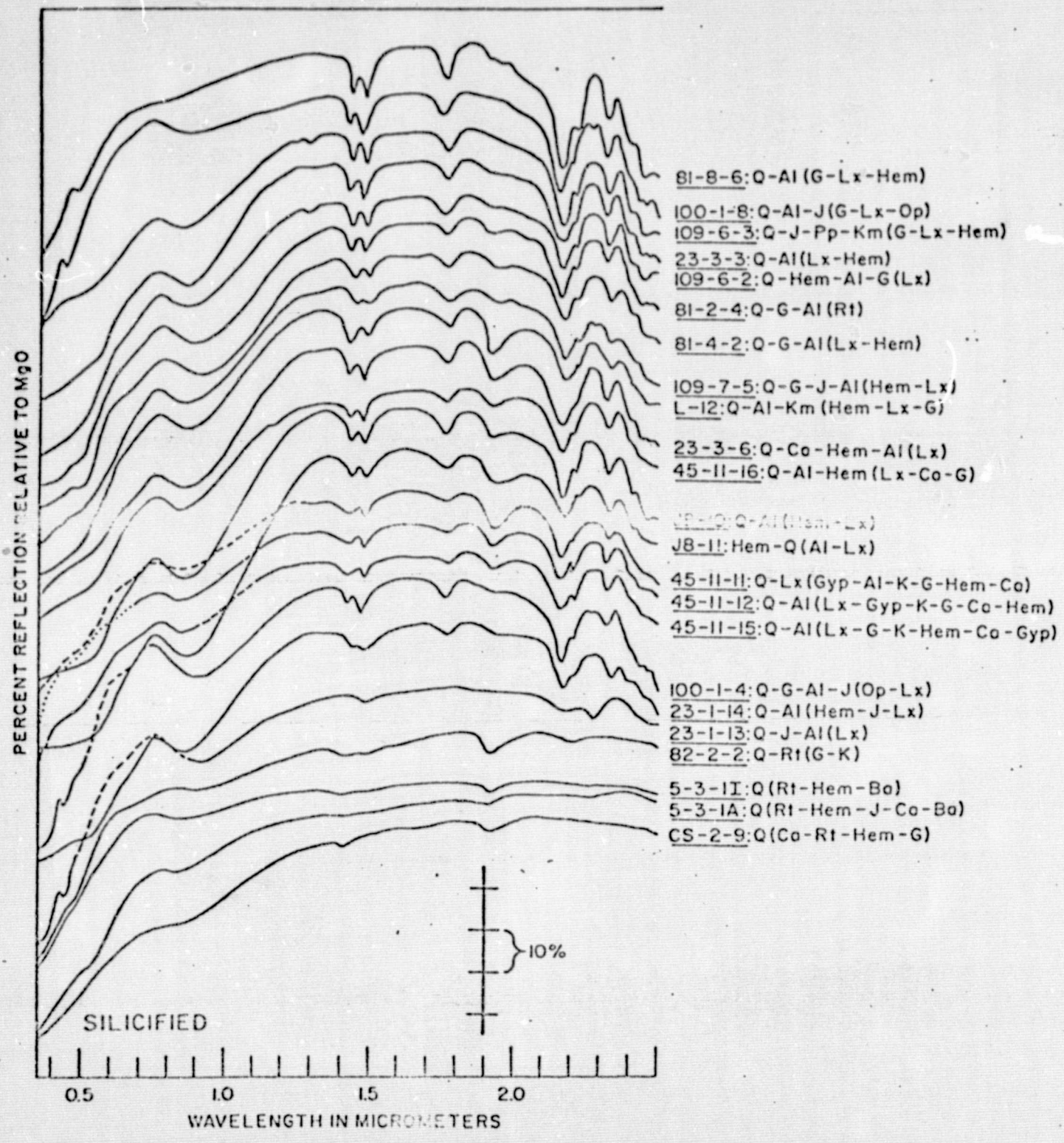
PERCENT REFLECTION RELATIVE TO MgO
81-8-6:Q-Al(G-Lx-Hem)
100-1-8:Q-Al-J(G-Lx-Op)
109-6-3:Q-J-Pp-Km(G-Lx-Hem)
23-3-3:Q-Al(Lx-Hem)
109-6-2:Q-Hem-Al-G(Lx)
81-2-4:Q-G-Al(Rt)
81-4-2:Q-G-Al(Lx-Hem)
109-7-5:Q-G-J-Al(Hem-Lx)
L-12:Q-Al-Km(Hem-Lx-G)
23-3-6:Q-Co-Hem-Al(Lx)
45-11-16:Q-Al-Hem(Lx-Co-G)
J8-11:Hem-Q(Al-Lx)
45-11-11:Q-Lx(Gyp-Al-K-G-Hem-Co)
45-11-12:Q-Al(Lx-Gyp-K-G-Co-Hem)
45-11-15:Q-Al(Lx-G-K-Hem-Co-Gyp)
100-1-4:Q-G-Al-J(Op-Lx)
23-1-14:Q-Al(Hem-J-Lx)
23-1-13:Q-J-Al(Lx)
82-2-2:Q-Rt(G-K)
5-3-11:Q(Rt-Hem-Ba)
5-3-1A:Q(Rt-Hem-J-Co-Ba)
CS-2-9:Q(Co-Rt-Hem-G)
10%
SILICIFIED
0.5
1.0
1.5
2.0
WAVELENGTH IN MICROMETERS

FIG 11

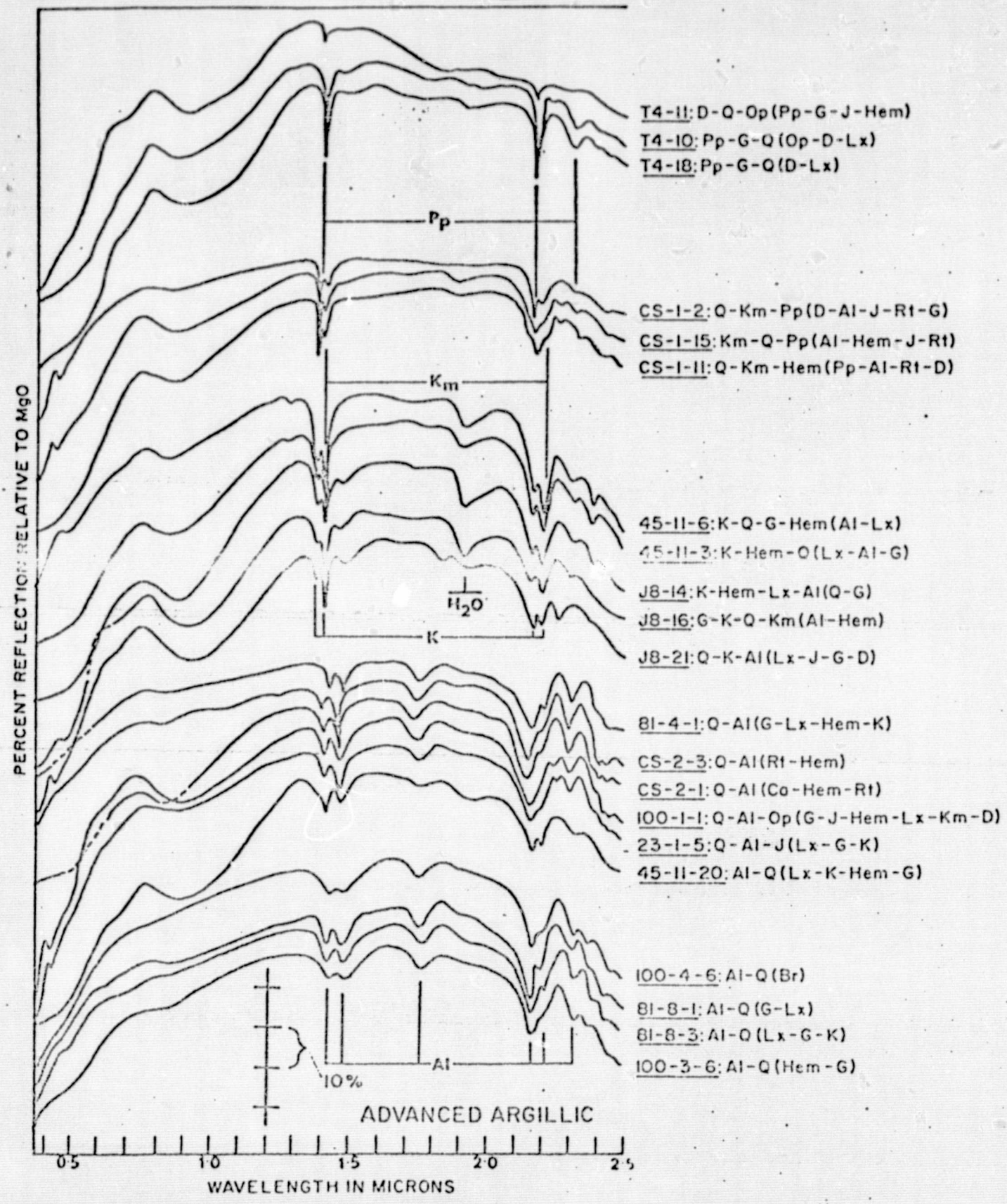

FIG 17

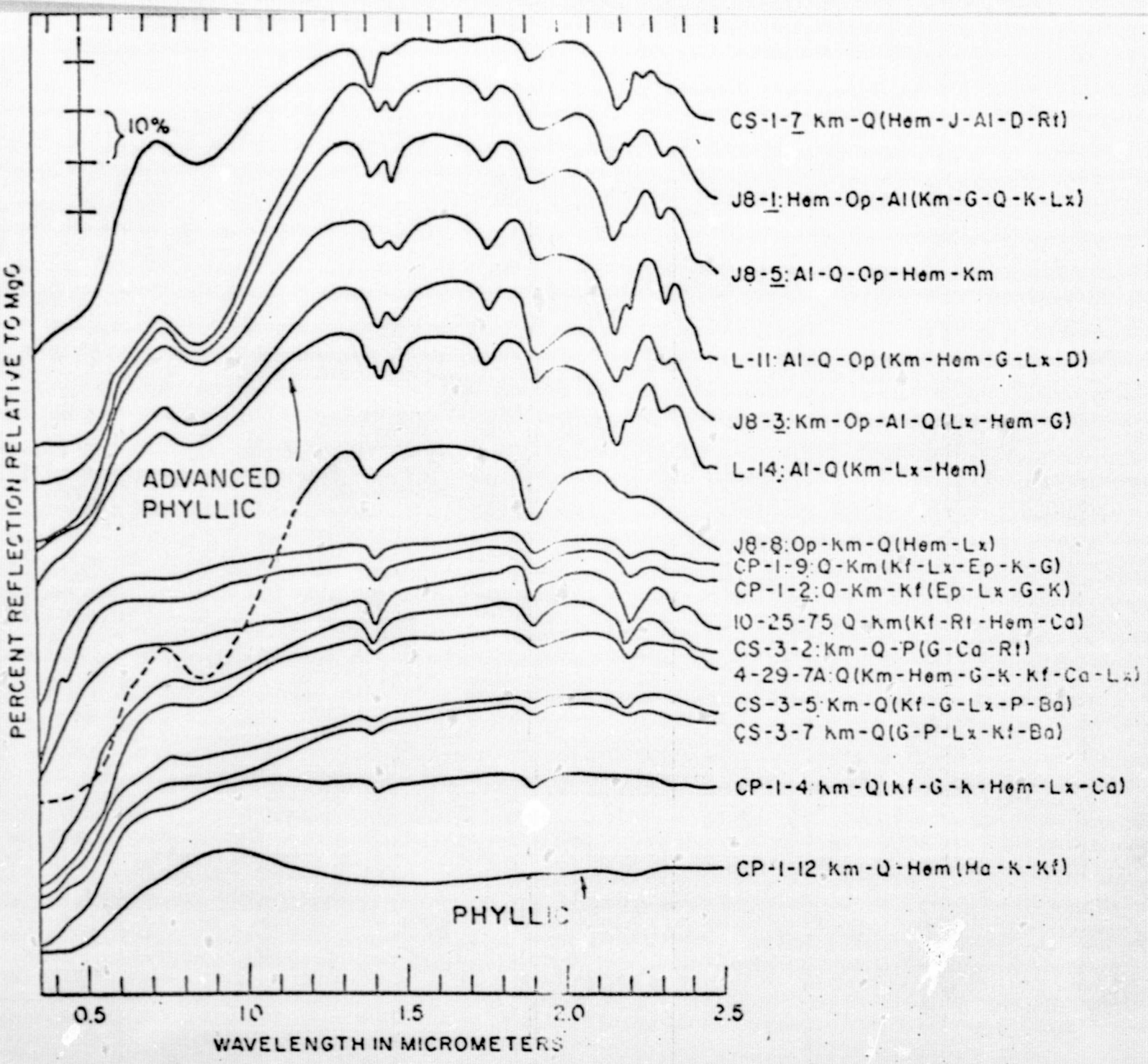
10%
CS-1-7 km-Q(Hem-J-Al-D-Rt)
J8-1:Hem-Op-Al(Km-G-Q-K-Lx)
J8-5:Al-Q-Op-Hem-Km
L-11:Al-Q-Op(Km-Hem-G-Lx-D)
J8-3:Km-Op-Al-Q(Lx-Hem-G)
L-14:Al-Q(Km-Lx-Hem)
ADVANCED PHYLLIC
J8-8:Op-Km-Q(Hem-Lx)
CP-1-9:Q-Km(Kf-Lx-Ep-K-G)
CP-1-2:Q-Km-Kf(Ep-Lx-G-K)
10-25-75 Q-Km(Kf-Rt-Hem-Ca)
CS-3-2:Km-Q-P(G-Ca-Rt)
4-29-7A:Q(Km-Hem-G-K-Kf-Ca-Lx)
CS-3-5:Km-Q(Kf-G-Lx-P-Ba)
CS-3-7 km-Q(G-P-Lx-Kf-Ba)
CP-1-4 km-Q(Kf-G-K-Hem-Lx-Ca)
CP-1-12 Km-Q-Hem(Ha-K-Kf)
PHYLLIC
PERCENT REFLECTION RELATIVE TO MgO
0.5
1.0
1.5
2.0
2.5
WAVELENGTH IN MICROMETERS

54

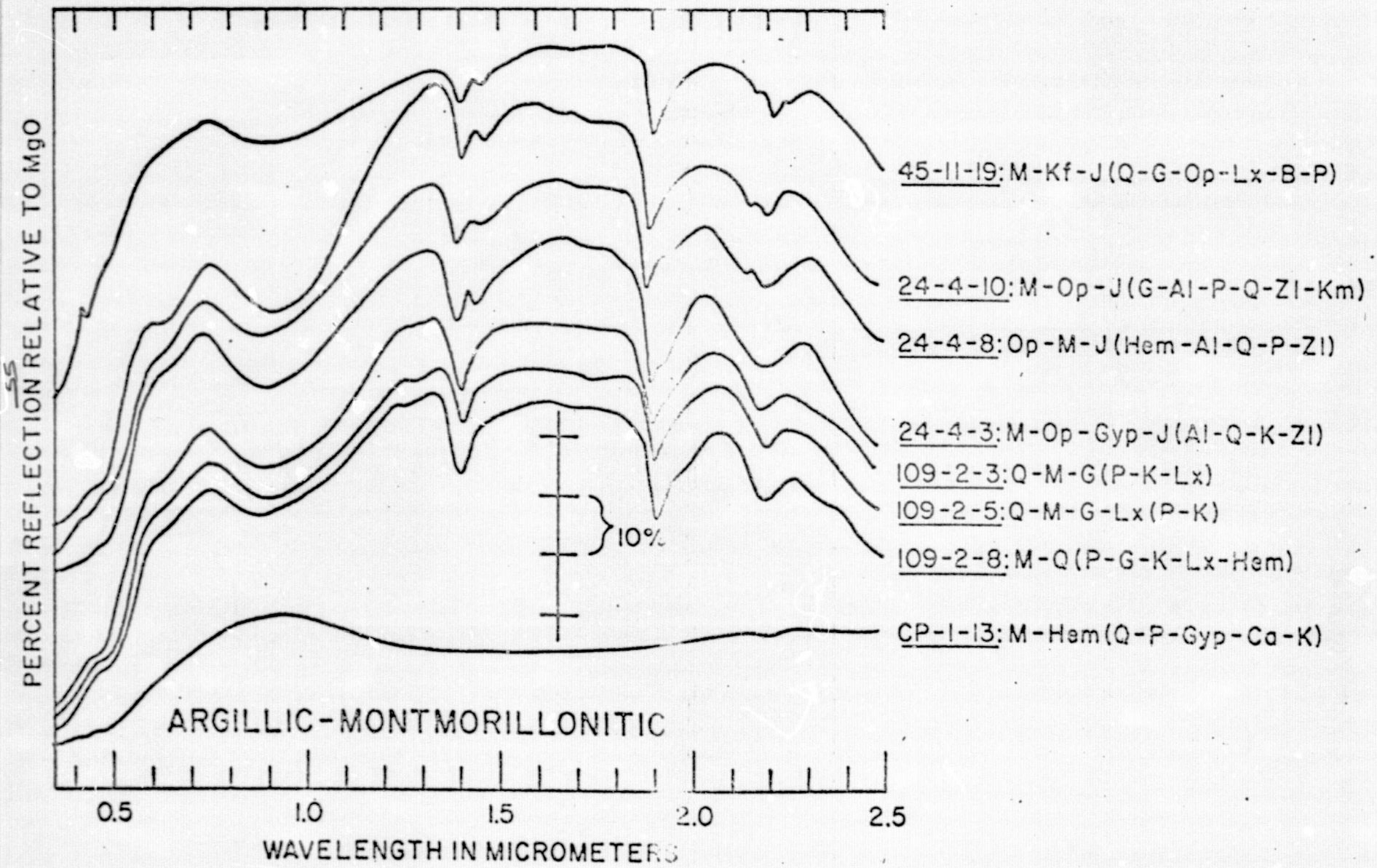
PERCENT REFLECTION RELATIVE TO MgO
55
45-11-19: M-Kf-J(Q-G-Op-Lx-B-P)
24-4-10: M-Op-J(G-Al-P-Q-Zl-Km)
24-4-8: Op-M-J(Hem-Al-Q-P-Zl)
24-4-3: M-Op-Gyp-J(Al-Q-K-Zl)
109-2-3: Q-M-G(P-K-Lx)
109-2-5: Q-M-G-Lx(P-K)
109-2-8: M-Q(P-G-K-Lx-Hem)
CP-1-13: M-Hem(Q-P-Gyp-Ca-K)
10%
ARGILLIC-MONTMORILLONITIC
0.5
1.0
1.5
2.0
2.5
WAVELENGTH IN MICROMETERS

FIG 14

36

FIG 15

ORIGINAL PAGE IS
OF POOR QUALITY